

Lipid biomarker distributions in Oligocene and Miocene sediments from the Ross Sea region, Antarctica

Duncan, Bella; McKay, Robert; Bendle, James; Naish, Timothy; Inglis, Gordon N.; Moossen, Heiko; Levy, Richard; Ventura, G. Todd; Lewis, Adam; Chamberlain, Beth; Walker, Carrie

DOI:

[10.1016/j.palaeo.2018.11.028](https://doi.org/10.1016/j.palaeo.2018.11.028)

License:

Creative Commons: Attribution-NonCommercial-NoDerivs (CC BY-NC-ND)

Document Version

Peer reviewed version

Citation for published version (Harvard):

Duncan, B, McKay, R, Bendle, J, Naish, T, Inglis, GN, Moossen, H, Levy, R, Ventura, GT, Lewis, A, Chamberlain, B & Walker, C 2019, 'Lipid biomarker distributions in Oligocene and Miocene sediments from the Ross Sea region, Antarctica: Implications for use of biomarker proxies in glacially-influenced settings', *Palaeogeography, Palaeoclimatology, Palaeoecology*, vol. 516, pp. 71-89.
<https://doi.org/10.1016/j.palaeo.2018.11.028>

[Link to publication on Research at Birmingham portal](#)

General rights

Unless a licence is specified above, all rights (including copyright and moral rights) in this document are retained by the authors and/or the copyright holders. The express permission of the copyright holder must be obtained for any use of this material other than for purposes permitted by law.

- Users may freely distribute the URL that is used to identify this publication.
- Users may download and/or print one copy of the publication from the University of Birmingham research portal for the purpose of private study or non-commercial research.
- User may use extracts from the document in line with the concept of 'fair dealing' under the Copyright, Designs and Patents Act 1988 (?)
- Users may not further distribute the material nor use it for the purposes of commercial gain.

Where a licence is displayed above, please note the terms and conditions of the licence govern your use of this document.

When citing, please reference the published version.

Take down policy

While the University of Birmingham exercises care and attention in making items available there are rare occasions when an item has been uploaded in error or has been deemed to be commercially or otherwise sensitive.

If you believe that this is the case for this document, please contact UBIRA@lists.bham.ac.uk providing details and we will remove access to the work immediately and investigate.

1 **Lipid biomarker distributions in Oligocene and Miocene sediments from**
2 **the Ross Sea region, Antarctica: Implications for use of biomarker proxies**
3 **in glacially influenced settings**

4 Bella Duncan^a, Robert McKay^a, James Bendle^b, Timothy Naish^a, Gordon N. Inglis^c, Heiko
5 Moossen^{b,d}, Richard Levy^c, G. Todd Ventura^{e,f}, Adam Lewis^g, Beth Chamberlain^{b,h}, Carrie Walker^{b,i}.

6

7 ^aAntarctic Research Centre, Victoria University of Wellington, P.O. Box, Wellington 6012, New
8 Zealand

9 ^bSchool of Geography, Earth and Environmental Sciences, University of Birmingham, Edgbaston,
10 Birmingham, B15 2TT, UK

11 ^cOrganic Geochemistry Unit, School of Chemistry and Cabot Institute, University of Bristol,
12 Cantock's Close, Bristol BS8 1TS, UK

13 ^dPresent address: Max Planck Institute for Biogeochemistry, P.O. Box 10 01 64, 07701 Jena,
14 Germany

15 ^eGeological and Nuclear Sciences, P.O. Box 30-368, Lower Hutt 5040, New Zealand

16 ^fPresent address: Department of Geology, Saint Mary's University, 923 Robie Street, Halifax, Nova
17 Scotia, B3H 3C3, Canada

18 ^gNorth Dakota State University, Fargo, North Dakota, 58105, USA

19 ^hPresent address: Department of Life Sciences, Imperial College London, Silwood Park Campus,
20 Buckhurst Road, BioAscot, Berkshire, SL5 7PY, UK

21 ⁱPresent address: School of Environment, Earth and Ecosystem Sciences, The Open University,
22 Milton Keynes, MK7 6AA, UK

23

24 Corresponding author: Bella Duncan, bella.duncan@vuw.ac.nz

25

26

27

28

29

30

31

32 **Abstract**

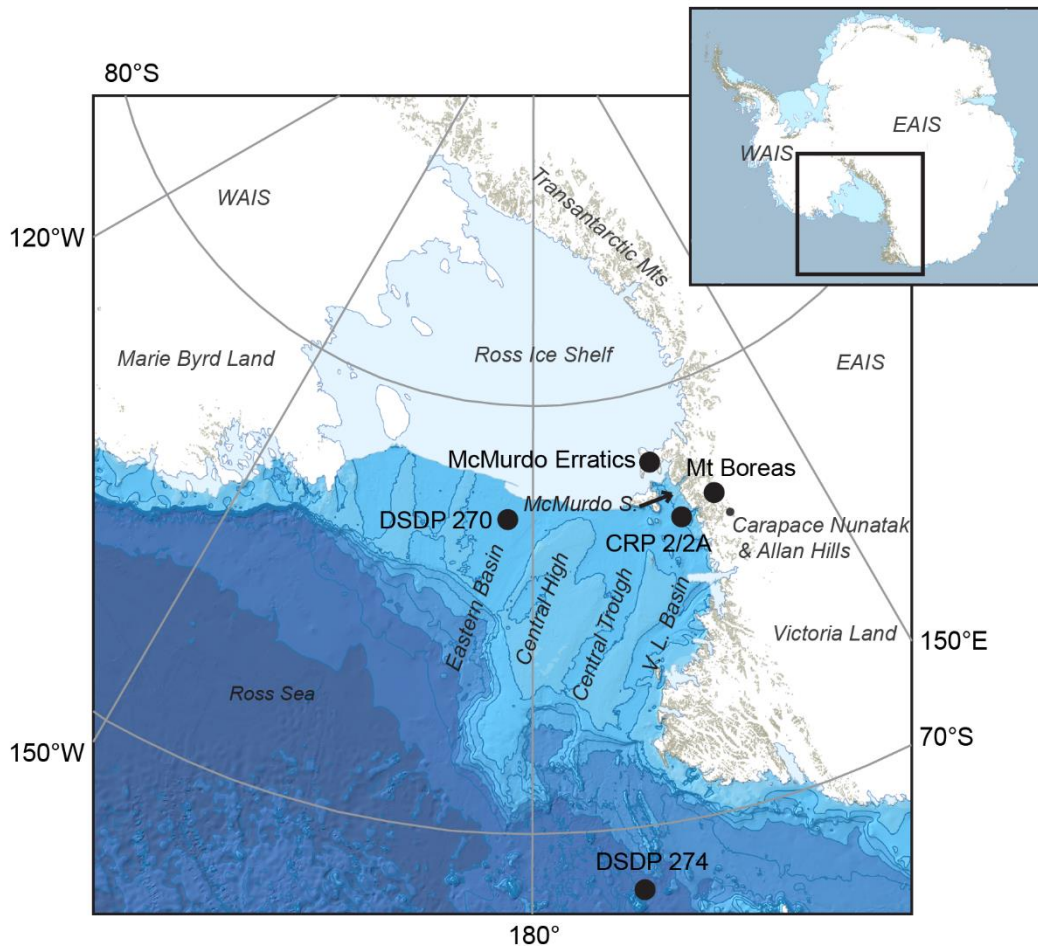
33 Biomarker-based climate proxies enable climate and environmental reconstructions for regions where
34 other paleoclimatic approaches are unsuitable. The Antarctic Cenozoic record consists of widely
35 varying lithologies, deposited in rapidly changing depositional settings, with large lateral variations.
36 Previous sedimentological and microfossil studies indicate that the incorporation of reworked older
37 material frequently occurs in these sediments, highlighting the need for an assessment of biomarker
38 distribution across a range of depositional settings and ages to assess the role reworking may have on
39 biomarker-based reconstructions. Here, we compare sedimentary facies with the distribution of *n*-
40 alkanes and hopanoids within a terrestrial outcrop, two glaciomarine cores and a deep sea core,
41 spanning the Late Oligocene to Miocene in the Ross Sea. Comparisons are also made with *n*-alkane
42 distributions in Eocene glacial erratics and Mesozoic Beacon Supergroup sediments, which are both
43 potential sources of reworked material. The dominant *n*-alkane chain length shifts from *n*-C₂₉ to *n*-C₂₇
44 between the Late Eocene and the Oligocene. This shift is likely due to changing plant community
45 composition and the plastic response of *n*-alkanes to climate cooling. Samples from glaciofluvial
46 environments onshore, and subglacial and ice-proximal environments offshore are more likely to display
47 reworked *n*-alkane distributions, whereas, samples from lower-energy, lacustrine and ice-distal marine
48 environments predominantly yield immature/contemporaneous *n*-alkanes. These findings emphasise
49 that careful comparisons with sedimentological and paleontological indicators are essential when
50 applying and interpreting *n*-alkane-based and other biomarker-based proxies in glacially-influenced
51 settings.

52 **Keywords:** Paleoclimate, Antarctica, *n*-alkanes, biomarkers, hopanoids, reworking

53 **1 Introduction**

54 In Antarctic sediments, traditional microfossil-based methods of reconstructing climate can be
55 challenging due to sparse distribution, low diversity of species, or poor preservation in sediments (i.e.
56 Askin and Raine, 2000; Strong and Webb, 2000; Scherer et al., 2007). In contrast, biomarkers
57 (molecular fossils preserved in the geological record) are relatively recalcitrant and have the potential
58 to provide environmental proxy information when other methods are challenging or unsuitable. To
59 date, only a few studies have employed biomarkers to investigate paleoclimate changes in Antarctica,
60 with most of these conducted in offshore settings (i.e. Feakins et al., 2012; McKay et al., 2012; Pross
61 et al., 2012; Bijl et al., 2013; Feakins et al., 2014; Levy et al., 2016; Rees-Owens et al., 2018). Such
62 work is challenging because Cenozoic outcrops exposed in Antarctica are sparse, and are represented
63 by relatively superficial and poorly-dated deposits of glacially derived tills, lacustrine and fluvial
64 deposits, with occasional marine and glaciomarine sediments (Hambrey and Barrett, 1993; Marchant
65 and Denton, 1996; Lewis et al., 2007; Lewis et al., 2008; Lewis and Ashworth, 2016). Sediments from
66 drillcores on the continental margin are usually glaciomarine in origin and provide better-dated

67 records of cyclical fluctuations of the Antarctic Ice Sheets (Barrett, 1989; Naish et al., 2001, 2009).
68 However, the variable lithologies in these sediments and the nature of their deposition mean that
69 reworking of older sediments and associated fossil material is potentially a significant issue (e.g.,
70 Kemp and Barrett, 1975; Askin and Raine, 2000; Prebble et al., 2006a).



71
72 *Fig. 1: Location of sample sites in the Ross Sea region of Antarctica. WAIS: West Antarctic*
73 *Ice Sheet, EAIS: East Antarctic Ice sheet, DSDP: Deep Sea Drilling Project, CRP: Cape Roberts*
74 *Project, McMurdo S.: McMurdo Sound, V.L. Basin: Victoria Land Basin. Base map from*
75 *Quantarctica GIS package, Norwegian Polar Institute.*

76 Here, lipid biomarkers (*n*-alkanes and hopanoids) are used to investigate how organic matter
77 varies between different lithologies and depositional environments in the Ross Sea region of
78 Antarctica. Specifically, we aim to assess whether lipid biomarkers represent organic material sourced
79 from organisms living contemporaneously with sediment deposition, or older organic material which
80 has been reworked into the sediment. Knowledge of potential reworking is critical for using and
81 interpreting biomarker-based paleoenvironmental proxies in glacially-influenced settings. Localities
82 and sediment drill cores were chosen to survey a range of depositional environments that together
83 form a transect from high elevation terrestrial deposits to the deep sea (Fig. 1). These include; (i) A

84 Middle Miocene (~14 Ma) lacustrine/fluviial sequence from a small mountain glacier catchment at Mt
85 Boreas in the Transantarctic Mountains. (ii) A Late Oligocene/Early Miocene glaciomarine sequence
86 in the shallow marine Cape Roberts Project 2/2A drill core, sampling a coastal sediment catchment
87 from an East Antarctic Ice Sheet (EAIS) outlet glacier. (iii) A deeper water Late Oligocene/Early
88 Miocene glaciomarine sequence in DSDP Site 270 sampling sediment sourced from now submerged
89 islands and ice caps in the central continental shelf of the Ross Sea, West Antarctica. (iv) An Early
90 Miocene to Late Miocene marine sequence from DSDP Site 274 from the Western Ross Sea abyssal
91 plain, sampling a wide sediment source catchment from both East and West Antarctica.

92 *1.1 Geological setting*

93 The western Ross Sea region of Antarctica is bounded by the Transantarctic Mountains
94 (TAM), which were uplifted in the early Cenozoic, with the bulk of their exhumation occurring before
95 the early Oligocene (Fitzgerald, 1994; Smellie, 2001). The basement rocks of the TAM are dominated
96 by Archean to mid-Paleozoic metasediments and intrusives (Allibone et al., 1993a; Allibone et al.,
97 1993b; Goodge et al., 2002). The Devonian to Triassic Beacon Supergroup overlies this basement
98 (Barrett, 1981). Lithologies vary through the sequence, with interbedded sandstones, shales,
99 conglomerates and coals deposited in a paleoenvironmental setting moving from shallow marine to a
100 terrestrial system of lakes, braided rivers and alluvial plains (Barrett, 1981). Plant macrofossils and
101 palynomorphs are common throughout the Beacon Supergroup (Barrett, 1981). In the early Jurassic,
102 as the Gondwana super-continent began to separate, the Beacon Supergroup was intruded by the
103 Ferrar Dolerite, resulting in extensive low grade thermal metamorphism (Barrett, et al., 1986). The
104 Jurassic Ferrar Group contains extrusive volcanic rocks with fossiliferous sedimentary interbeds
105 containing terrestrial microfossil assemblages (e.g. Ribecai, 2007).

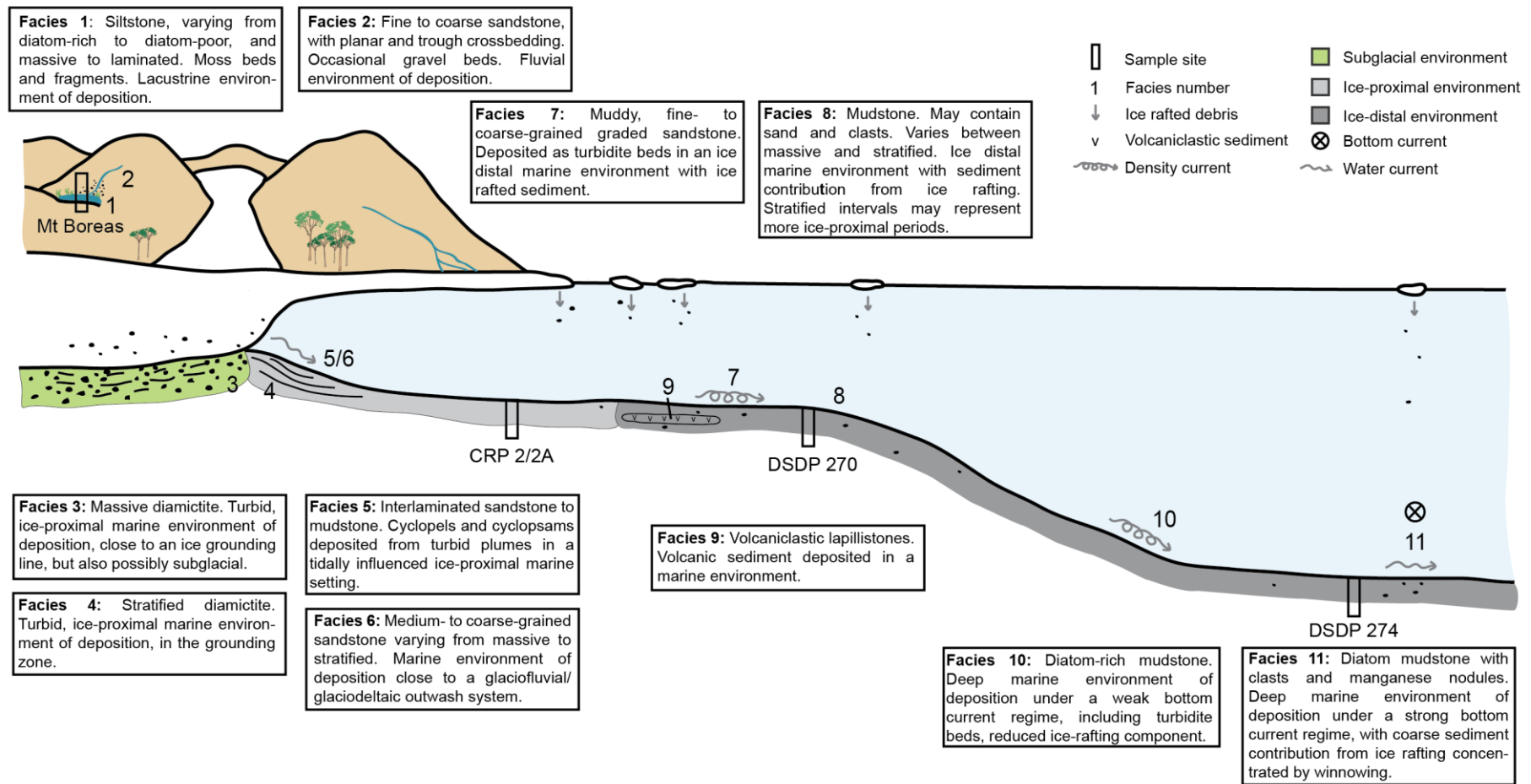
106 Scattered sedimentary outcrops and the basaltic McMurdo Volcanic Group form the Cenozoic
107 geology of the TAM (Marchant and Denton, 1996; Fielding et al., 2006; Martin et al, 2010). A
108 significant Cenozoic sedimentary unit distributed throughout the TAM is the Sirius Group, which
109 comprises glacial and non-glacial sediments with well-preserved fossil woody vegetation, leaf
110 material and peat beds, deposited in terrestrial and proximal marine environments (Hambrey and
111 Barrett, 1993; Francis and Hill, 1996; Barrett, 2013). Scattered Early Miocene to Holocene veneers of
112 glacial tills, colluvium and lacustrine deposits are dispersed through the TAM (Marchant and Denton,
113 1996; Lewis et al., 2007; Lewis et al., 2008; Lewis and Ashworth, 2016). Eocene to Pliocene glacial
114 erratics are found in the McMurdo region (Harwood and Levy, 2000). Much of what is currently
115 known about Cenozoic Antarctic climate is based on seismic stratigraphy and continental margin
116 drilling. Infill of sedimentary basins in the Ross Sea potentially began as early as the Late Cretaceous,
117 with sediment accumulation continuing through the Cenozoic (Cooper et al., 1987; De Santis et al.,
118 1995; Luyendyk et al., 2001; Decesari et al., 2007; Wilson and Luyendyk, 2009). Continental margin

119 drill cores from the Ross Sea contain successions of subglacial, glaciomarine and marine sediments
120 reflecting the cyclical advance and retreat of the Antarctic Ice Sheets (i.e. Barrett, 1989; Naish et al.,
121 2001; Naish et al., 2009; McKay et al., 2009; Levy et al., 2016).

122 **2 Methods**

123 *2.1 Site description*

124 This work utilises samples from: (i) The McMurdo glacial erratics from the Mt Discovery and
125 Minna Bluff region (Fig. 1), which yield marine and terrestrial micro- and macrofossils of mid-late
126 Eocene age and are interpreted as being deposited in coastal-terrestrial and nearshore marine
127 environments, under ice-free conditions (Harwood and Levy, 2000). (ii) Mid-Miocene terrestrial,
128 fossil-bearing strata from Mt Boreas in the Olympus Range, which record the last known vestige of
129 vegetation in the TAM before the Dry Valleys transitioned from wet- to cold-based glaciation at high
130 altitudes (1,425 m) (Fig. 1) (Lewis et al., 2008). (iii) Oligocene/Early Miocene glaciomarine
131 sediments obtained from the Cape Roberts Project core CRP-2/2A from the Victoria Land continental
132 slope of Antarctica (Fig. 1) (Cape Roberts Science Team, 1999). (iv) A Late Oligocene to Early
133 Miocene glaciomarine sequence of sediments from DSDP Site 270, drilled on the continental shelf in
134 the central Ross Sea in 1973 and re-described in 2015 (Fig. 1) (The Shipboard Scientific Party, 1975a;
135 Kraus, 2016). (v) An Early to Late Miocene succession of ice-distal diatom-rich silty clay sediments
136 from DSDP 274 on the lower continental rise in the northwestern Ross Sea (68°59.81'S,
137 173°25.64'W) (Fig. 1) (The Shipboard Scientific Party, 1975b). Figure 2 schematically describes the
138 sampling sites and facies used in this study.



139

140 *Fig. 2. Schematic representation of Oligocene and Miocene environments of deposition in the Ross Sea Region, and their associated sedimentary*
 141 *facies. Sample sites are placed in their representative depositional setting.*

142

143 2.2 Bulk analysis

144 Unless already desiccated, samples were freeze dried for 48 h prior to sample work up. All
145 samples were homogenised to a powder using a Retsch 200 mixer mill.

146 Pyrolysis measurements for total organic carbon (TOC) were made using a Weatherford
147 laboratories Source Rock Analyzer at GNS Science on ~100 mg of powdered sediment. The
148 pyrolysis program was set with the sample crucible entering the pyrolysis oven where it was held
149 isothermal at 300 °C for 3 mins under a continuous stream of He carrier gas using a 100 ml/min flow
150 rate. This was followed by a 25 °C/min ramp to 650 °C. The S1 and S2 signal intensities were
151 recorded with a FID operated under a 65 ml/min stream of H₂ gas and 300 ml/min air. The pyrolysis
152 cycle was then followed by an oxidation cycle performed at 630 °C for 20 mins during which time the
153 oven and crucible were flushed with dry air at 250 ml/min. The generated carbon monoxide and
154 carbon dioxide gases were measured by the instrument's IR cells. All sample sequences were run
155 with three IFP 160000 analytical standard replicates (from Vinci Technologies, Institut Français du
156 Pétrole) placed at the beginning, middle and end of each sample sequence.

157 2.3 Lipid biomarker analyses

158 Organic geochemical work-up, gas chromatograph (GC)-flame ionization detector (FID) and
159 GC-Mass Spectrometer (MS) analyses was performed in the Birmingham Molecular Climatology
160 Laboratory (BMC), University of Birmingham. Lipids were extracted from ~10-15 g of homogenised
161 sediment by ultrasonic extraction using dichloromethane (DCM):methanol (3:1). The total lipid
162 extract was fractionated by silica gel chromatography using *n*-hexane, *n*-hexane:DCM (2:1), DCM,
163 and methanol to produce four separate fractions, the first of which contained the aliphatic saturated
164 and unsaturated hydrocarbons (e.g. *n*-alkanes, steranes and hopanes). Procedural blanks were also
165 analysed to ensure the absence of laboratory contaminants.

166 The aliphatic hydrocarbon fractions were analysed on an Agilent 7890B series GC, equipped
167 with a 7639ALS autosampler, a BP5-MS column (SGE Analytical Science, 60 m × 0.32 mm × 0.25
168 μm) and an FID, using hydrogen (H₂) as a carrier gas. Compound separation was achieved by using
169 the following temperature program: the oven was held at 70 °C for 1 min, then heated to 120 °C at 30
170 °C/min, and then to 320 °C with 3 °C/min, where it was held for 20 mins. GC-Mass spectrometry
171 (GC-MS) was performed using an Agilent 7890B GC, coupled to an Agilent 5977A Mass Selective
172 Detector (MSD). The same capillary column and temperature program was used throughout the
173 analyses for consistent compound separation. Helium (He) was used as a carrier gas. Samples were
174 bracketed with an external standard containing known abundances of certain *n*-alkanes to allow
175 identification and quantification of *n*-alkanes (average standard deviation of ± 7.6%). *n*-Alkane peaks

176 were integrated in Agilent OpenLAB Data Analysis Version A.01.01 - Build 1.93.0. Relationships
177 between *n*-alkane indices were investigated using Pearson's correlation coefficients and assessed as
178 statistically significant when $p < 0.05$. Hopanes and hopenes were identified based upon published
179 spectra, characteristic mass fragments and retention times (e.g. Rohmer et al., 1984; Sessions et al.,
180 2013; Inglis et al., 2018) and integrated using GC-MS.

181 2.4 Biomarker indices

182 *n*-Alkanes of specific carbon chain lengths are known to be derived from discrete biological
183 sources. Algae and some photosynthetic bacteria typically produce dominantly *n*-C₁₇, with lesser
184 amounts of *n*-C₁₅ and *n*-C₁₉ (Clark and Blumer, 1967; Han and Calvin, 1969; Cranwell et al., 1987).
185 Other species of bacteria, including non-photosynthetic bacteria often demonstrate an even carbon
186 number preference between *n*-C₁₂ and *n*-C₂₂, commonly with high *n*-C₁₆ and *n*-C₁₈ (Han and Calvin,
187 1969; Grimalt and Albaigés, 1987). Non-emergent aquatic plants and *Sphagnum* mosses show
188 enhanced production of *n*-C₂₃ and *n*-C₂₅ (Baas et al., 2000; Ficken et al., 2000; Pancost et al., 2002;
189 Bingham et al., 2010). Long chain *n*-alkanes (*n*-C₂₅ and higher), usually with a high odd-over-even
190 predominance, are most abundant in the epicuticular waxes on leaves and stems of terrestrial higher
191 plants (Eglinton and Hamilton, 1963). *n*-Alkanes are also derived from the early diagenetic alteration
192 of saturated and unsaturated aliphatic alcohols, ketones, esters, and di- or triterpenic acids (i.e. Tissot
193 and Welte, 1984; Meyers and Ishiwatari 1993). Once deposited, *n*-alkanes may undergo microbial or
194 geochemical alteration, modifying their distributions (Grimalt et al., 1985).

195 The source and maturity of higher molecular weight *n*-alkanes can be characterised by their
196 carbon preference index (CPI):

$$197 \quad CPI = \frac{1}{2} \left(\frac{\sum_{odd}(n-C_{25-33})}{\sum_{even}(n-C_{24-32})} + \frac{\sum_{odd}(n-C_{25-33})}{\sum_{even}(n-C_{26-34})} \right) \quad (1)$$

198 Most modern sediments with terrestrially sourced organic matter have an odd-over-even
199 predominance of long chained *n*-alkanes (*n*-C₂₅ to *n*-C₃₄) and CPI values > 1 (Bray and Evans, 1961;
200 Eglinton and Hamilton, 1963). A survey of modern leaf wax material demonstrates that a CPI of $> 1-2$
201 is a reasonable threshold value indicative of relatively unmodified terrestrial plant material (Bush and
202 McInerney, 2013). Sediments containing CPI values of < 1 usually indicate either exposure to elevated
203 burial temperatures great enough to cause hydrocarbon cracking, or an input of organic matter that has
204 been altered by diagenetic or catagenetic processes (Bray and Evans, 1961). Some sediments will also
205 display an unresolved complex mixture (UCM), represented by a hump in the baseline of a gas
206 chromatogram due to the co-elution of unresolved compounds (Gough and Rowland, 1990; Gough et
207 al., 1992). UCMs can be especially prominent in biodegraded petroleum, in which microbial
208 degradation of the more abundant aliphatic components leads to increased concentrations of the more
209 recalcitrant, branched and cyclic compounds (Gough and Rowland, 1990; Gough et al., 1992). In

210 recent sediments, *n*-alkanes have a lower susceptibility to microbial degradation than most other types
211 of organic matter as they lack functional groups, but studies on peat and lake sediments suggest that
212 microbial degradation does occur (Meyers and Ishiwatari, 1993; Lehtonen and Ketola, 1993). Shorter
213 chain lengths appear more degradable than longer chain lengths, and microbial degradation can result
214 in a decrease in CPI (Meyers and Ishiwatari, 1993; Lehtonen and Ketola, 1993).

215 Average chain length (ACL) indicates the dominant *n*-alkane in a given carbon number range
216 (Poynter et al., 1989; Schefuß et al., 2003):

$$217 \quad ACL = \frac{\sum(C_{odd\ 25-33} \cdot x_{odd\ 25-33})}{(x_{odd\ 25-33})} \quad (2)$$

218 Where $C_{odd\ 25-33}$ represents the carbon number of the odd chain length *n*-alkanes, and $x_{odd\ 25-33}$
219 represents the concentrations of the odd *n*-alkanes in the sample. ACL is influenced by a number of
220 factors. Higher ACLs are typical of warmer, tropical regions, whilst lower ACLs are more commonly
221 observed from cooler, temperate regions, indicating that ACL could be related to air temperature
222 (Gagosian and Peltzer, 1986; Poynter et al., 1989; Dodd and Afzal-Rafii, 2000; Kawamura et al.,
223 2003; Bendle et al., 2007; Vogts et al., 2009; Bush and McInerney, 2015). Other studies have
224 suggested that aridity has a strong control on ACL, with the synthesis of longer *n*-alkanes in more arid
225 environments providing plants with a more efficient wax coating to restrict water loss (Dodd et al.,
226 1998; Dodd and Afzal-Rafii, 2000; Schefuß et al., 2003; Calvo et al., 2004; Zhou et al., 2005;
227 Moossen et al., 2015). ACL is also strongly controlled by the contributing vegetation, with large inter-
228 and intra-species variation in *n*-alkane distributions (i.e. Vogts et al., 2009; Bush and McInerney,
229 2013; Feakins et al., 2016). Variation in average chain length through time therefore reflects the
230 interplay of two key factors: climate-driven plastic response of *n*-alkanes to temperature and/or aridity
231 within a plant community; or changes to the composition of the plant community, often in response to
232 climate (Bush and McInerney, 2013).

233 Hopanes and hopenes are C_{27} to C_{35} pentacyclic triterpenoids derived from a wide range of
234 bacteria (Rohmer et al., 1984; Talbot and Farrimond, 2007). Hopanes are ubiquitous across a variety
235 of depositional settings, and in both modern and ancient sediments (Ourisson and Albrecht, 1992). In
236 modern sediments, hopanes are mostly present in the biological $17\beta,21\beta(H)$ configuration (although
237 there are exceptions; see Inglis et al., 2018). In sediments, with increasing diagenesis, hopanes
238 undergo stereochemical transformations and the biologically-derived $17\beta,21\beta(H)$ -hopanoid is
239 transformed into the more thermally stable $17\beta,21\alpha(H)$ and $17\alpha,21\beta(H)$ -stereoisomers (Mackenzie et
240 al., 1980; Peters and Moldowan, 1991). With increasing maturation, extended hopanoids ($>C_{30}$) also
241 undergo isomerisation at the C-22 position. As such, hopanoids are frequently used to reconstruct
242 thermal maturity (Mackenzie et al., 1980; Seifert and Moldowan, 1980; Peters and Moldowan, 1991;
243 Farrimond et al., 1998), where decreasing $\beta\beta/(\alpha\beta+\beta\alpha+\beta\beta)$ indices and increasing $22S/(22R + 22S)$
244 values indicate increasing thermal maturity. The ratio of C_{27} $18\alpha(H)$ -trisnorhopane II (Ts) to C_{27}

245 17 α (H)-trishnorhopane (Tm) is also commonly used as a maturity parameter, as Tm is less stable
246 during catagenesis than Ts (Seifert and Moldowan, 1978).

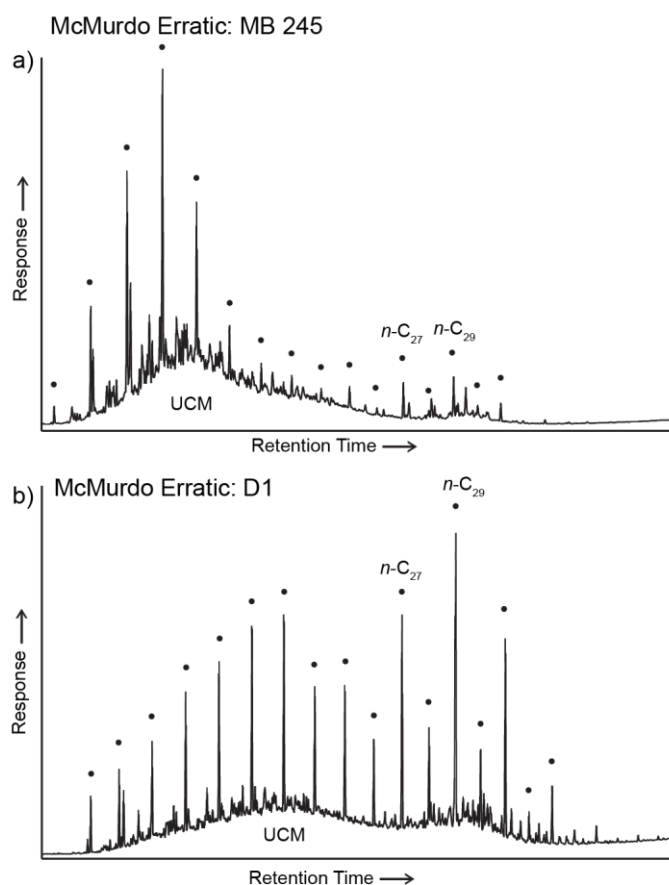
247 **3 Results**

248 *3.1 Facies compilation*

249 In order to compare results between sites, an internally consistent facies scheme was
250 developed based on published facies descriptions for each sample site (Fig. 2). The McMurdo erratics
251 were not included, as the context and relationship between these samples is uncertain. Instead these
252 samples were labelled by lithofacies as described by Levy and Harwood (2000) (Supplementary table
253 1). Samples from Mt Boreas were assigned facies based on descriptions from Lewis et al. (2008).
254 Facies for CRP 2/2A were developed based on descriptions of Fielding et al. (2000). Facies for DSDP
255 270 were assigned using descriptions of Kraus (2016), and based on previous models of glaciomarine
256 facies successions (Fielding et al, 2000; Powell and Cooper, 2002; McKay et al., 2009). For DSDP
257 274, facies were determined by using interpretations from The Shipboard Scientific Party (1975b),
258 Frakes (1975) and Whittaker and Müller (2006).

259 *3.2 McMurdo erratics*

260 Six Mid- Late Eocene sediment samples from the McMurdo erratics suite were analysed for
261 *n*-alkanes, sourced from a range of lithofacies (Levy and Harwood, 2000) (Supplementary table 1).
262 Three of the samples (E214, MB245 and E215) are dominated by the *n*-C₁₇ to *n*-C₂₀ short chained *n*-
263 alkanes underlain by a UCM (Fig. 3). Samples D1, E219 and MTD95 have bimodal profiles,
264 dominated by \sim *n*-C₂₀ to *n*-C₂₃ underlain by small a UCM, and a series of longer *n*-alkanes with a
265 mode at \sim *n*-C₂₉ (Fig. 3). In all samples, *n*-C₂₉ is the dominant long-chained *n*-alkane, in contrast to
266 younger strata investigated in this study usually dominated by *n*-C₂₇. The ratio between these two
267 chain lengths has been described at all sites to investigate its variance at other localities. The CPI from
268 the McMurdo Erratics ranges from 1.8 to 5.5 (avg. 2.8). ACL varies from 27.9 to 28.7 (avg. 28.2),
269 whilst the ratio of the *n*-C₂₉ *n*-alkane to *n*-C₂₇ ranges from 1.01 to 1.64 (avg. 1.26). The erratics
270 contain total abundances of *n*-alkanes ranging from 83 μ g/gTOC to 1579 μ g/gTOC, at an average of
271 406 μ g/gTOC.

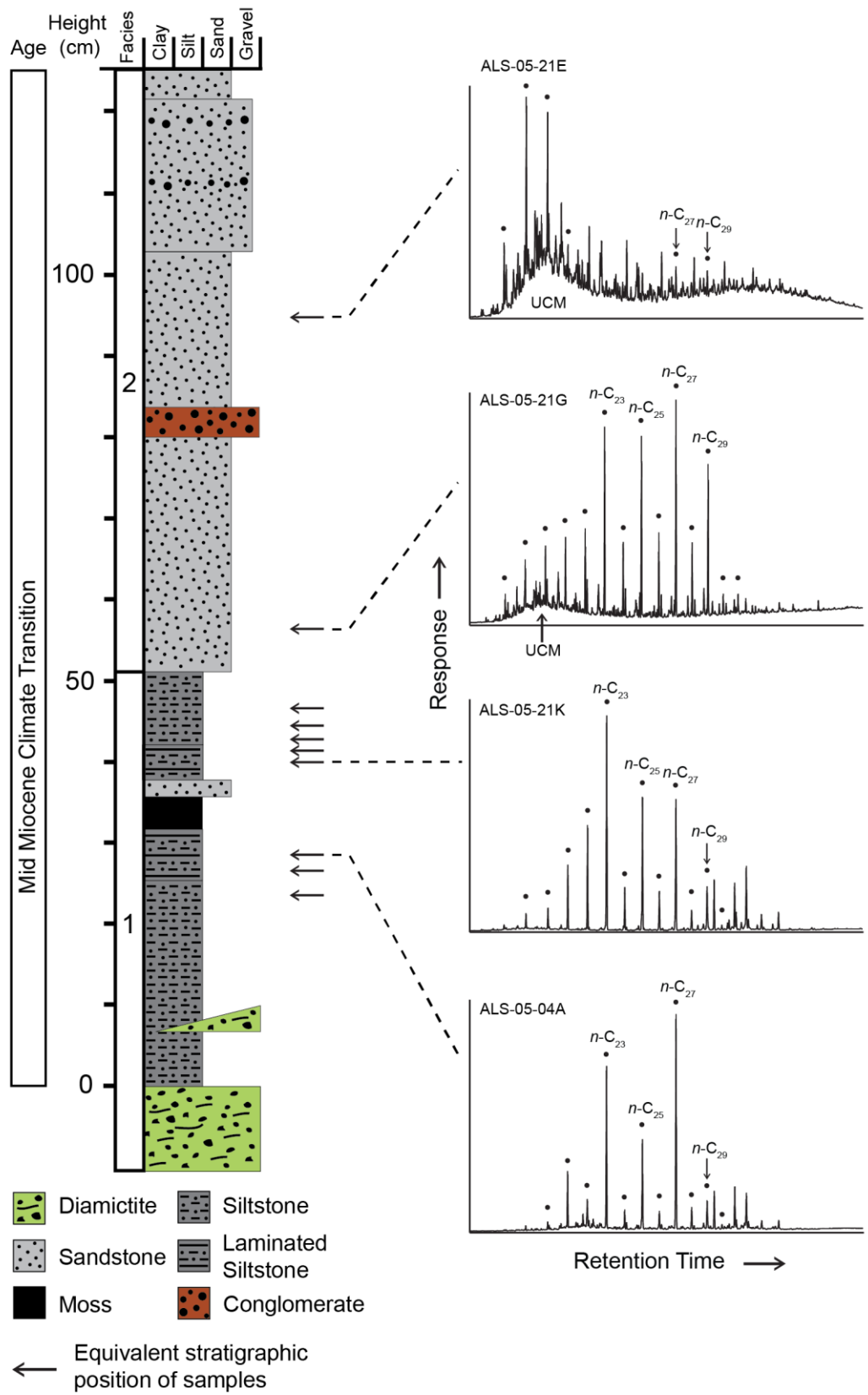


272

273 *Fig. 3. Representative GC-FID-chromatograms of two samples of the McMurdo erratics.*
 274 *Filled circles above peaks indicate n-alkanes, with the n-C₂₇ and n-C₂₉ labelled. UCM: unresolved*
 275 *complex mixture.*

276 3.3 Mt Boreas

277 12 sediment samples from Mt Boreas were analysed for *n*-alkanes (Supplementary table 1)
 278 Samples from Mt Boreas are typically dominated by long chained *n*-alkanes, particularly *n*-C₂₃, *n*-C₂₅
 279 and *n*-C₂₇ (Fig. 4). Some samples display small UCMs, usually underlying ~*n*-C₁₉ to *n*-C₂₀. Samples
 280 were collected from three different sites within a topographic depression which held a small alpine
 281 line, from units that are correlatable to the stratigraphic column shown in Figure 4 (Lewis et al.,
 282 2008). The total abundance of *n*-alkanes at these sites ranges between 4.5 µg/gTOC to 762 µg/gTOC,
 283 at an average of 206.5 µg/gTOC. The CPI of the long-chained *n*-alkanes ranges from 1.7 to 5.9 (avg.
 284 3.4), whilst ACL varies from 26.2 to 27.4 (avg. 26.9). The ratio of the *n*-C₂₉ *n*-alkane to *n*-C₂₇ varies
 285 from 0.15-0.97 (avg. 0.55), indicating that the *n*-C₂₇ dominates the *n*-C₂₉ in all samples from these
 286 sites (Supplementary table 1).



287

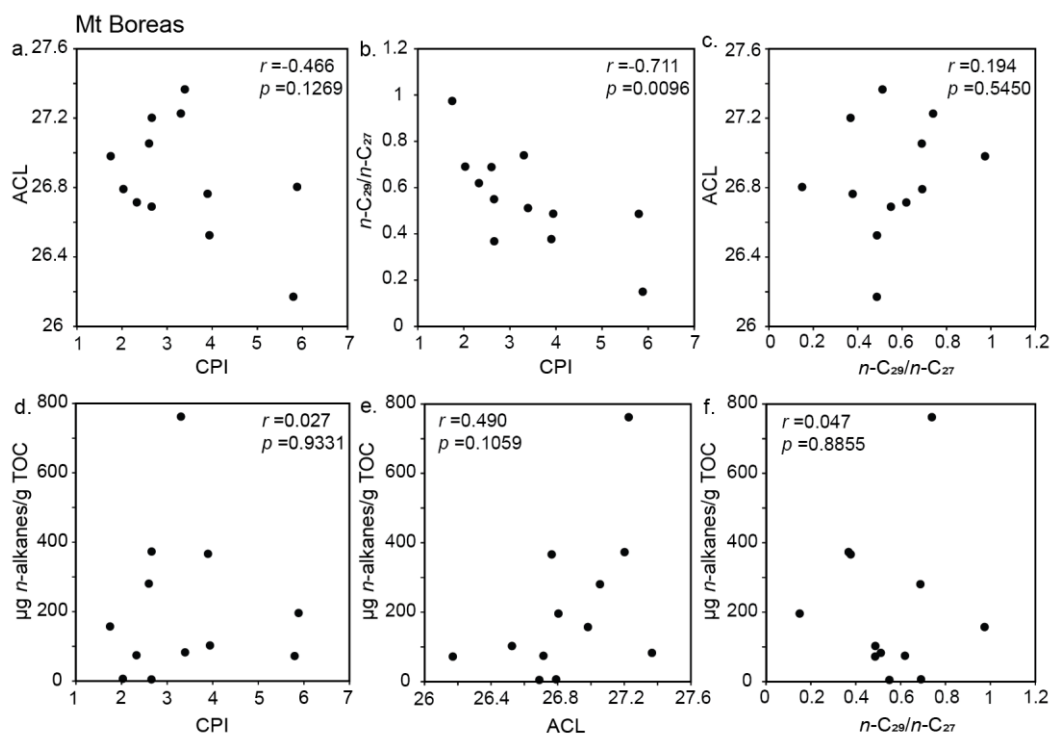
288

289

Fig. 4. Stratigraphic column from a site at Mt Boreas (after Lewis et al., 2008) with the equivalent stratigraphic positions of representative GC-FID-chromatograms of samples. Filled

290 circles above peaks indicate *n*-alkanes, with the *n*-C₂₇ and *n*-C₂₉ labelled. Facies numbers are
 291 described in Fig. 2. UCM: unresolved complex mixture.

292 Pearson's correlation coefficients were estimated for each *n*-alkane variable compared to
 293 other *n*-alkane variables from these sites. Only two variables demonstrate a statistically significant
 294 correlation to each other; the ratio of *n*-C₂₉/*n*-C₂₇ typically decreases with increasing CPI ($r = 0.711$, p
 295 $= 0.0096$) (Fig. 5). Samples from fluvial Facies 2 typically display lower CPI, and higher ACL and *n*-
 296 C₂₉/*n*-C₂₇ values than those from lacustrine Facies 1, although it is noted that the Facies 2 is only
 297 represented by two samples (Fig. 6). Both fluvial and lacustrine samples show similar average total
 298 abundances of *n*-alkanes.

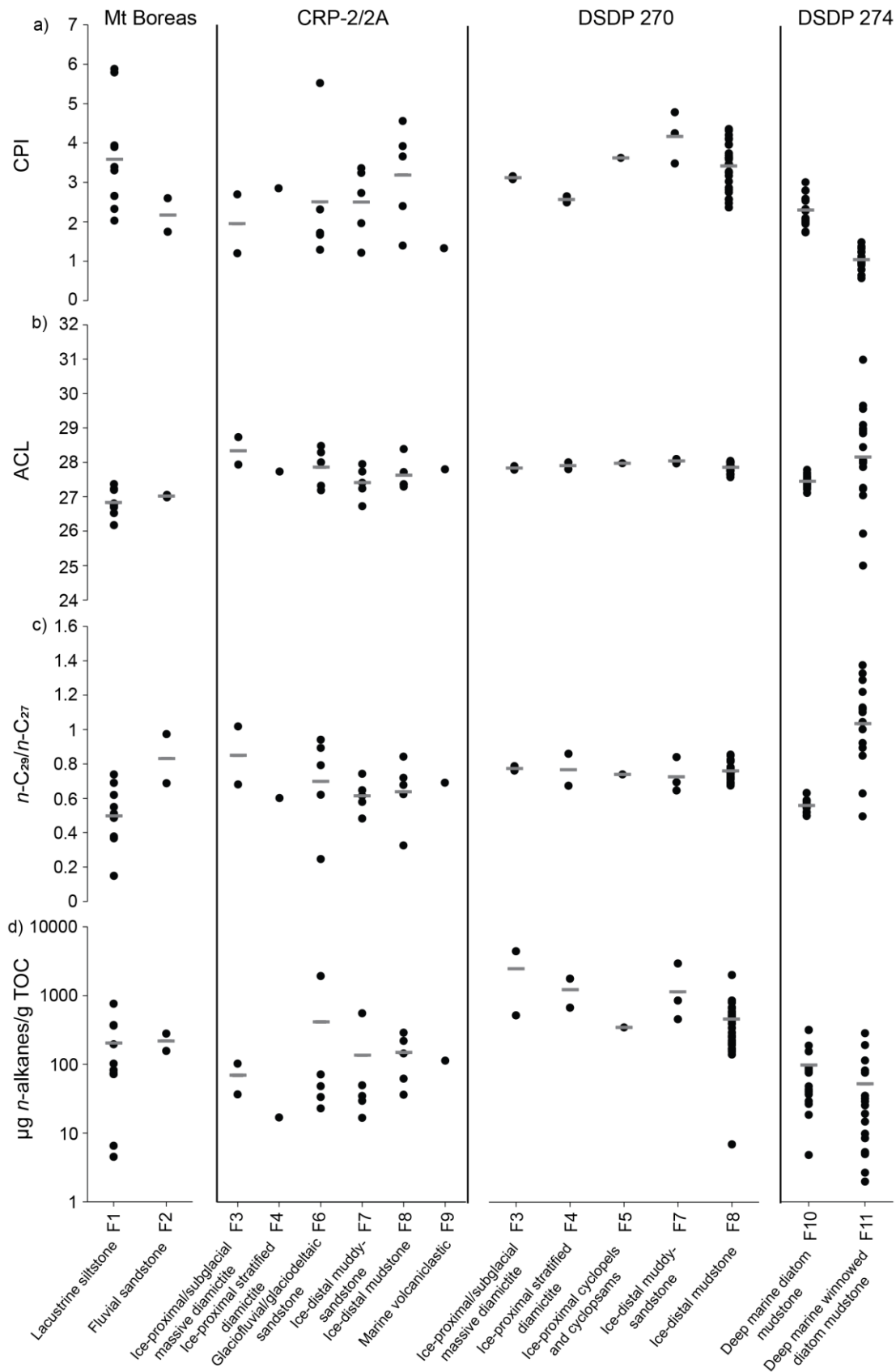


299

300 *Fig. 5. Scatter plots of samples from Mt Boreas; a) CPI and ACL; b) CPI and $n\text{-C}_{29}/n\text{-C}_{27}$; c)*
 301 *$n\text{-C}_{29}/n\text{-C}_{27}$ and ACL; d) CPI and the total abundance of *n*-alkanes ($\mu\text{g } n\text{-alkanes/g TOC}$); e) ACL and*
 302 *the total abundance of *n*-alkanes ($\mu\text{g } n\text{-alkanes/g TOC}$) and f) $n\text{-C}_{29}/n\text{-C}_{27}$ and the total abundance of*
 303 **n*-alkanes ($\mu\text{g } n\text{-alkanes/g TOC}$).*

304 Three samples representing typical *n*-alkane distributions from the site were also analysed for
 305 additional biomarkers (Supplementary table 2). In two samples (ALS-05-21N and ALS-05-04C),
 306 hopanoids were abundant and the distribution was dominated by 17 β (H)-trisnorhopane (C₂₇) and
 307 17 β ,21 β (H)-norhopane (C₂₉). Both samples are characterised by high $\beta\beta/(\alpha\beta+\beta\alpha+\beta\beta)$ ratios (0.82 to
 308 0.86) and indicate low thermal maturity. Within sample ALS-05 21O, hopanoids were weak and the
 309 distribution was dominated by thermally-mature C₂₇ to C₃₅ hopanes. This sample was characterised by

310 a low $\beta\beta/(\alpha\beta+\beta\alpha+\beta\beta)$ ratio (0.07) and high C22S/C22R+C22S ratio (0.58) and therefore indicate high
 311 thermal maturity.



312

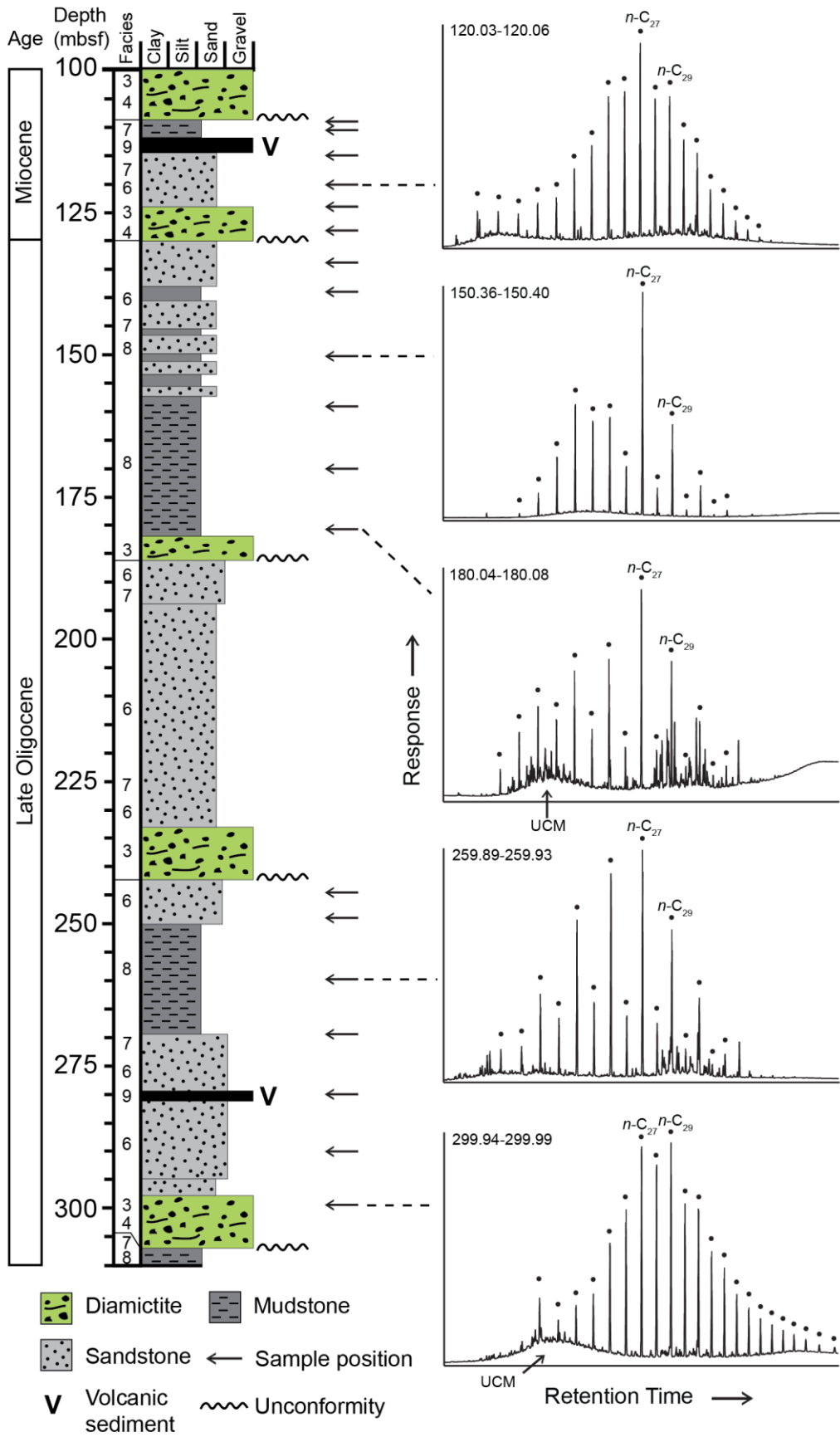
313 *Fig. 6: Distributions of n-alkane variables across different facies from Mt Boreas, CRP-2/2A,*
314 *DSDP 270 and DSDP 274; a) CPI, b) ACL, c) n-C₂₉/n-C₂₇ and d) the total abundance of n-alkanes*
315 *(µg n-alkanes/g TOC). Grey bars represent average values for each facies. Description of facies in*
316 *Fig. 2.*

317 3.4 Cape Roberts Project 2/2A

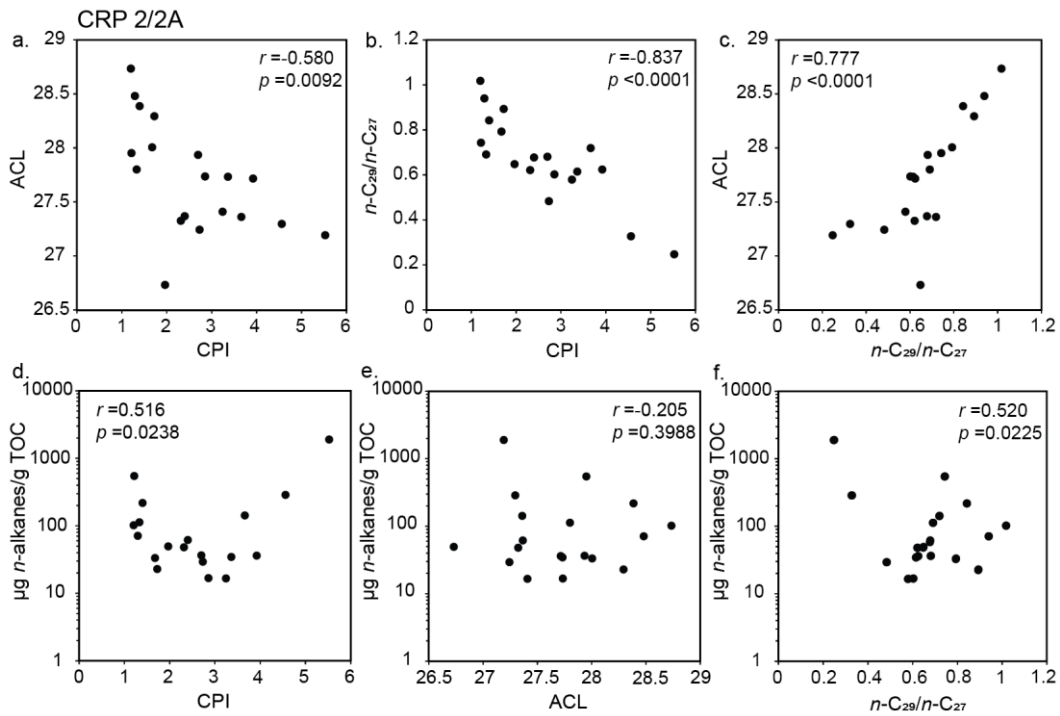
318 Long chained n-alkanes typically dominate samples from CRP 2/2A (Fig. 7). The n-C₂₃, n-C₂₅
319 and n-C₂₇ are usually the most abundant homologs, with n-C₂₇ often the most prominent of these. In
320 some samples n-alkanes elute with a UCM, which is usually centred between n-C₁₉ and n-C₂₃. The
321 total abundance of n-alkanes is highly variable from sample to sample, ranging from 16.6 µg/gTOC to
322 1893.0 µg/gTOC, averaging 197.6 µg/gTOC. CPI also varies over a wide range, from 1.2-5.5 (avg.
323 2.6), whilst ACL ranges from 26.7-28.7 (avg. 27.7). The ratio of the n-C₂₉ n-alkane to n-C₂₇ varies
324 from 0.25-1.02 (avg. 0.67) (Supplementary table 1).

325 Pearson's correlation coefficient estimations show statistically significant correlations
326 between several n-alkane variables. The strongest correlations exist between CPI and n-C₂₉/n-C₂₇ ($r =$
327 $0.837, p < 0.0001$) and ACL and n-C₂₉/n-C₂₇ ($r = 0.777, p < 0.0001$), with a weaker correlation
328 between CPI and ACL ($r = 0.580, p = 0.0091$). Figure 8 shows that at both high and low values of
329 CPI and n-C₂₉/n-C₂₇, the total abundance of n-alkanes increases, with weak correlations between these
330 variables ($r = 0.516, p = 0.0238$ and $r = 0.520, p = 0.0225$, respectively). Most facies contain a range
331 of both high and low values of CPI, with the highest average CPI in the low-energy marine mudstones
332 of facies 8 (Fig. 6). Facies 6, 7 and 8 also have broad ranges of ACL and n-C₂₉/n-C₂₇, with the lowest
333 average ACL and n-C₂₉/n-C₂₇ in the poorly sorted sandstones of facies 7, while facies 3, consisting of
334 massive diamictites, has the highest average ACL and n-C₂₉/n-C₂₇. Two samples containing a much
335 higher concentration of n-alkanes than other samples in the facies skew the averages for facies 6 and
336 7. Without these outliers, facies 8 contains the highest average total abundance of n-alkanes.

337 Additional biomarkers were investigated in two samples, with a range of C₂₇–C₃₂ hopanes and
338 C₂₇–C₃₀ hopenes were present (Supplementary table 2). The dominant compound was 17β,21β(H)-
339 bishomohopane (C₃₂) or 17α,21β(H)-hopane (C₃₀) and samples were characterised by low-to-
340 moderate ββ/(αβ+βα+ββ) ratios (0.45 to 0.65). As such, these samples are characterised by relatively
341 low thermal maturity.



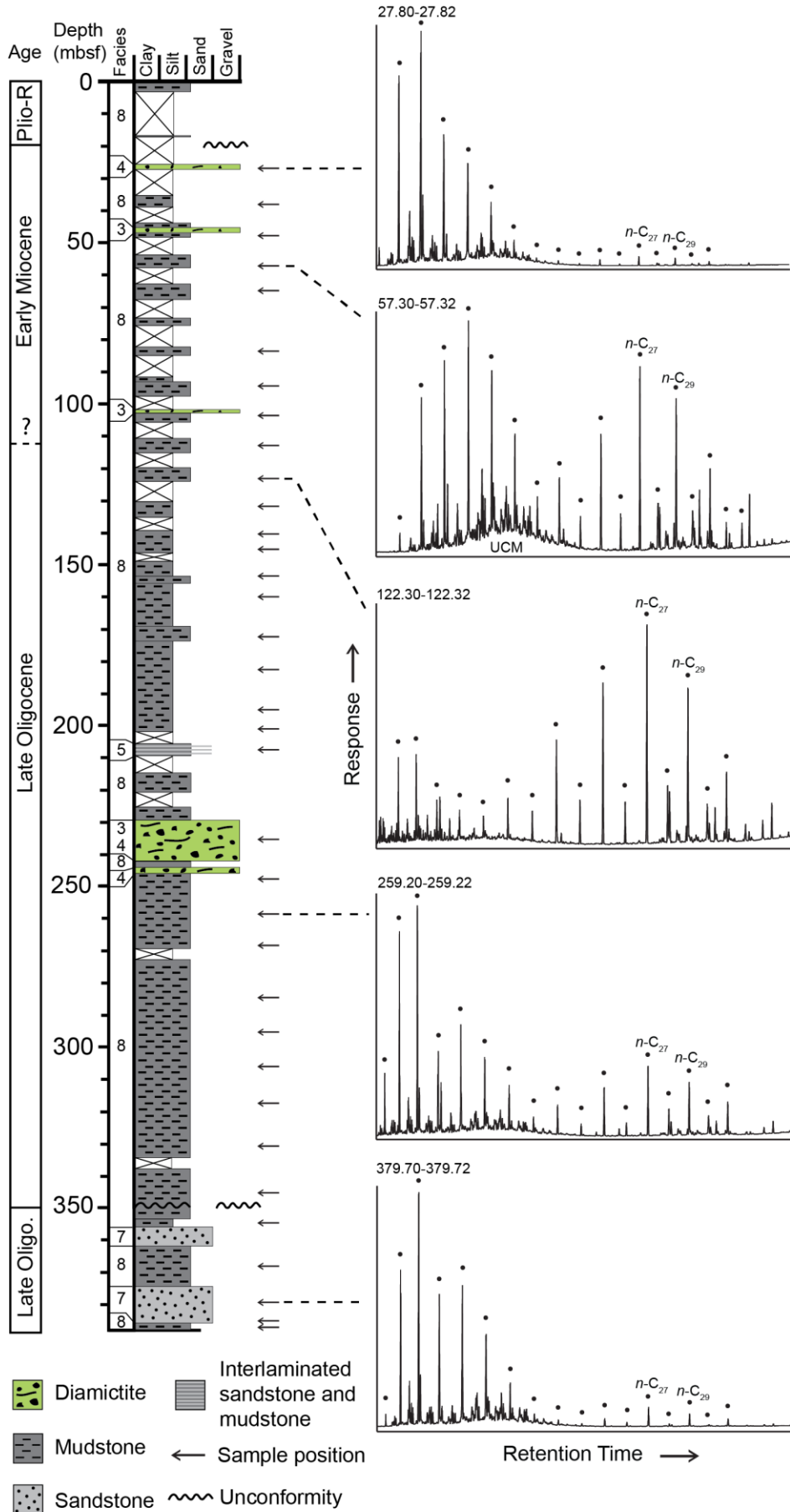
343 *Fig. 7. Stratigraphic column from CRP 2/2A with the stratigraphic positions of representative*
 344 *GC-FID-chromatograms of samples. Filled circles above peaks indicate n-alkanes, with the n-C₂₇ and*
 345 *n-C₂₉ labelled. Simplified facies groupings are labelled, and are described in table 1. UCM:*
 346 *unresolved complex mixture.*



347
 348 *Fig. 8. Scatter plots of samples from CRP 2/2A; a) CPI and ACL; b) CPI and n-C₂₉/n-C₂₇; c)*
 349 *n-C₂₉/n-C₂₇ and ACL; d) CPI and the total abundance of n-alkanes (μg n-alkanes/g TOC); e) ACL and*
 350 *the total abundance of n-alkanes (μg n-alkanes/g TOC) and f) n-C₂₉/n-C₂₇ and the total abundance of*
 351 *n-alkanes (μg n-alkanes/g TOC).*

352 3.4 DSDP 270

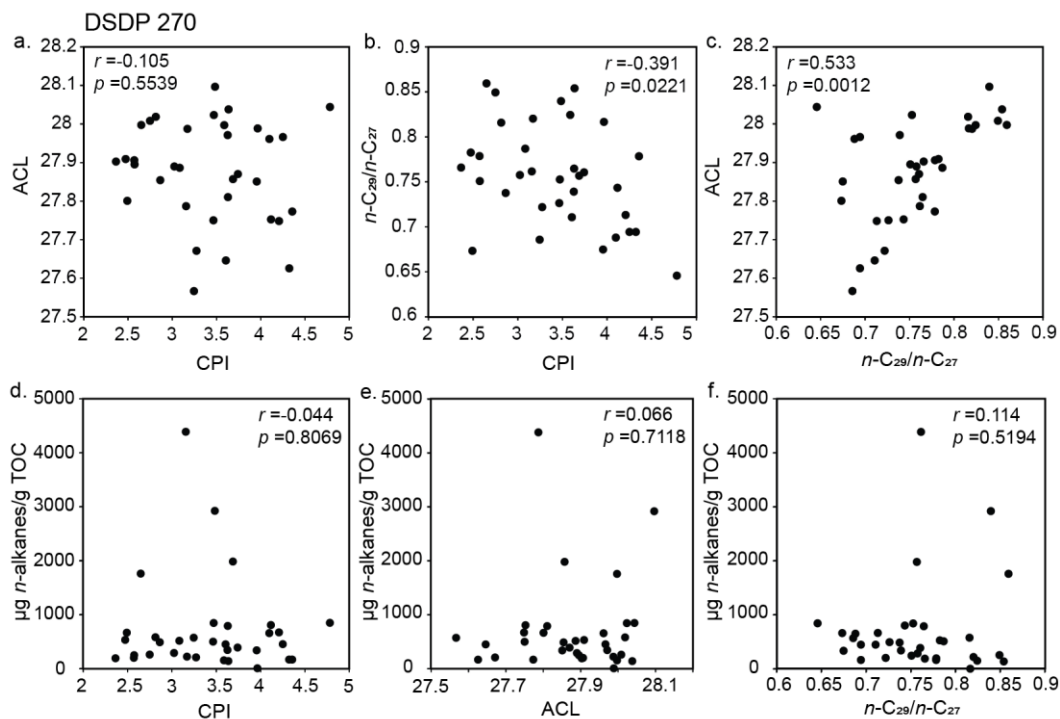
353 Samples from DSDP 270 typically display bimodal *n*-alkane distributions with a peak at *n*-C₁₇
 354 or *n*-C₁₉ and another peak *n*-C₂₇ (Fig. 9). Shorter chained *n*-alkanes (> *n*-C₂₀) are usually more
 355 abundant than the long chained homologs, and in four samples from the lowest sampled section of the
 356 core, long chained *n*-alkanes were not detected. Some samples display a small UCM underlying ~*n*-
 357 C₂₀ and *n*-C₂₁. CPI of the long chained *n*-alkanes ranges from 2.4-4.8 (avg. 3.4). ACL varies from
 358 27.6-28.1 (avg. 27.9), whilst the ratio of *n*-C₂₉ to *n*-C₂₇ ranges from 0.65-0.86 (avg. 0.76). The
 359 samples have an average total abundance of *n*-alkanes of 680.92 μg/gTOC (Supplementary table 1).



361 *Fig. 9. Stratigraphic column from DSDP 270 with the stratigraphic positions of*
 362 *representative GC-FID-chromatograms of samples. Filled circles above peaks indicate n-alkanes,*
 363 *with the n-C₂₇ and n-C₂₉ labelled. Simplified facies groupings are labelled, and are described in table*
 364 *1. UCM: unresolved complex mixture.*

365 Pearson's correlation coefficients show no particularly strong correlations between n-alkane
 366 variables. Increasing n-C₂₉/n-C₂₇ with decreasing CPI is very weakly correlated ($r = 0.391$, $p =$
 367 0.0221), with a slightly stronger correlation existing between decreasing n-C₂₉/n-C₂₇ with decreasing
 368 ACL ($r = 0.533$, $p = 0.0012$) (Fig. 10). When grouped by facies, facies 7 demonstrates the highest
 369 average CPI, and facies 4 contains the lowest average CPI (Fig. 6). Facies 7 shows the highest
 370 average ACL and lowest average n-C₂₉/n-C₂₇, but most facies display similar ACL and n-C₂₉/n-C₂₇
 371 values. Most facies also contain a similar total abundance of n-alkanes, with the highest average
 372 abundance in facies 3.

373 Two samples with representative n-alkane distributions were analysed for additional
 374 biomarkers (Supplementary table 2). Samples contained a range of C₂₇–C₃₂ hopanes and C₂₇–
 375 C₃₀ hopenes. The dominant compounds were 17β(H)-trisnorhopane (C₂₇), 17α,21β(H)-hopane
 376 (C₃₀), 17β,21β(H)-homohopane (C₃₁). Both samples were characterised by high ββ/(αβ+βα+ββ) ratios
 377 (0.69 to 1.00) and indicate low thermal maturity.



378

379 *Fig. 10. Scatter plots of samples from DSDP 270; a) CPI and ACL; b) CPI and n-C₂₉/n-C₂₇;*
 380 *c) n-C₂₉/n-C₂₇ and ACL; d) CPI and the total abundance of n-alkanes ($\mu\text{g n-alkanes/g TOC}$); e) ACL*

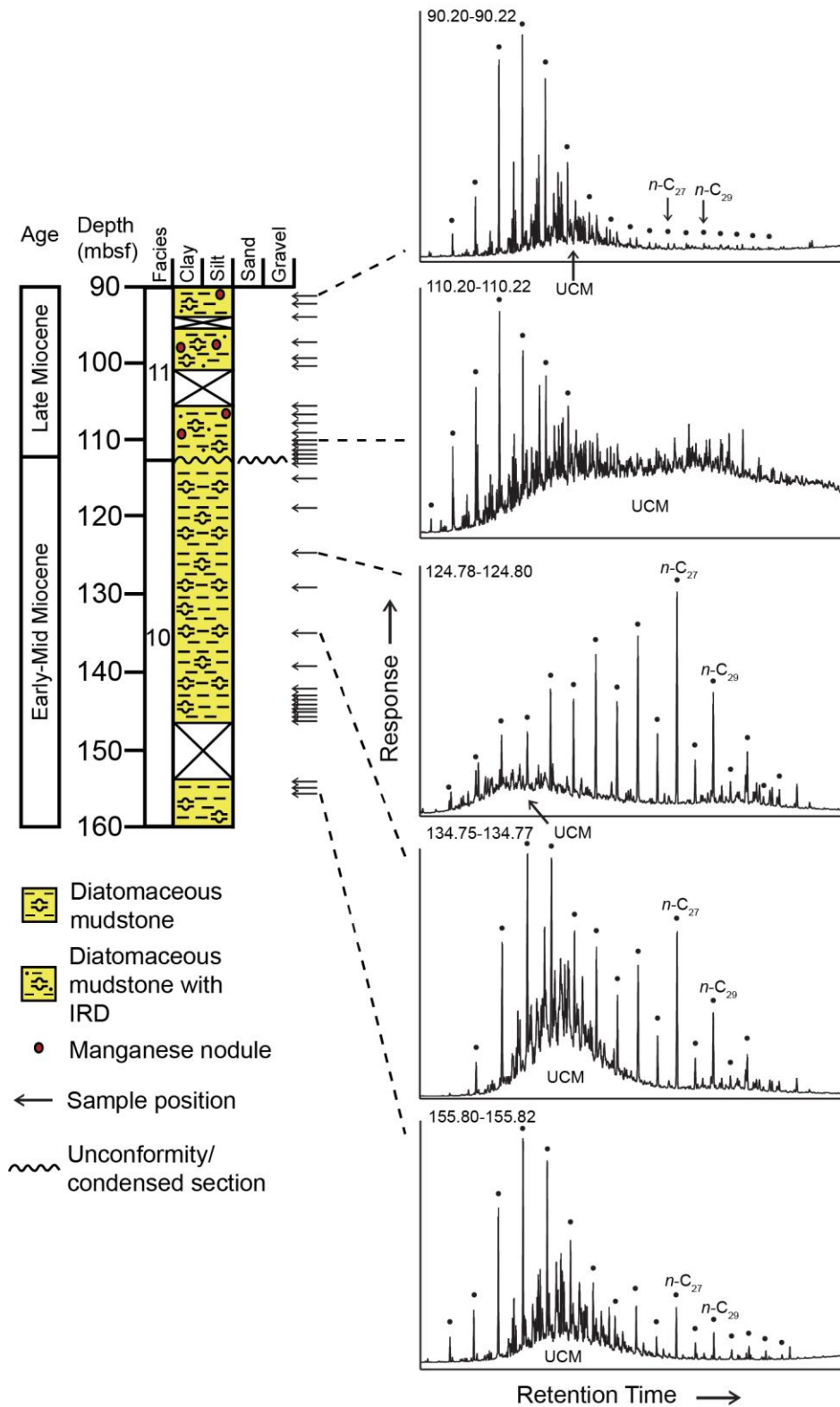
381 and the total abundance of *n*-alkanes ($\mu\text{g } n\text{-alkanes/g TOC}$) and f) $n\text{-C}_{29}/n\text{-C}_{27}$ and the total
382 abundance of *n*-alkanes ($\mu\text{g } n\text{-alkanes/g TOC}$).

383 3.5 DSDP 274

384 Samples taken from above 115m had variable, or even absent, quantities of *n*-alkanes (Fig.
385 11). Samples usually contained significant UCMs, which typically dominated the signal, and *n*-
386 alkanes did not display a common dominant *n*-alkane. Samples below 115m were usually bimodal in
387 distribution, with a dominant *n*-alkane peak around $n\text{-C}_{19}$, $n\text{-C}_{20}$ or $n\text{-C}_{21}$, underlain by a UCM, and
388 another peak centred at $n\text{-C}_{27}$. CPI ranges from 0.6 to 3.0 (avg. 1.6), whilst ACL ranges from 25 to
389 31.0 (avg. 27.8). The ratio of $n\text{-C}_{29}$ to $n\text{-C}_{27}$ varies from 0.50 to 1.37 (avg. 0.80). The total abundance
390 of *n*-alkanes averages 72.7 $\mu\text{g/gTOC}$, with a range of 2.7 $\mu\text{g/gTOC}$ to 316.6 $\mu\text{g/gTOC}$
391 (Supplementary table 1).

392 Pearson's correlation coefficients show the strongest correlations exist between CPI and *n*-
393 $\text{C}_{29}/n\text{-C}_{27}$ ($r = 0.809$, $p < 0.0000$), and ACL and $n\text{-C}_{29}/n\text{-C}_{27}$ ($r = 0.825$, $p < 0.0000$) (Fig. 12). Weak
394 correlations exist between the total abundance of *n*-alkanes and the other three variables considered;
395 CPI, ACL and $n\text{-C}_{29}/n\text{-C}_{27}$ ($r = 0.350$, $p = 0.0461$; $r = 0.396$, $p = 0.0224$; $r = 0.389$, $p = 0.0338$
396 respectively). Only one combination, CPI and ACL, does not indicate a statistically significant
397 correlation, as ACL becomes much more variable at low CPIs. Facies 11 has significantly lower CPI
398 and higher $n\text{-C}_{29}/n\text{-C}_{27}$ than facies 10 (Fig. 6). ACL is much more variable in facies 11, and on
399 average higher, while the total abundance of *n*-alkanes is on average lower than facies 10.

400 One sample from facies 11 was analysed for additional biomarkers (Supplementary table 2).
401 The sample contained a range of thermally mature $\text{C}_{27}\text{--C}_{35}$ hopanes. The dominant compounds were
402 $17\alpha,21\beta(\text{H})\text{-norhopane}$ (C_{29}) and $17\alpha,21\beta(\text{H})\text{-hopane}$ (C_{30}). This sample was characterised by low
403 $\beta\beta/(\alpha\beta+\beta\alpha+\beta\beta)$ ratios (0), high $\text{C}_{22}\text{S}/\text{C}_{22}\text{R}+\text{C}_{22}\text{S}$ ratios (0.57) and moderate $\text{T}_s/\text{T}_s+\text{T}_m$ ratio (0.31).
404 Collectively, this indicates high thermal maturity.



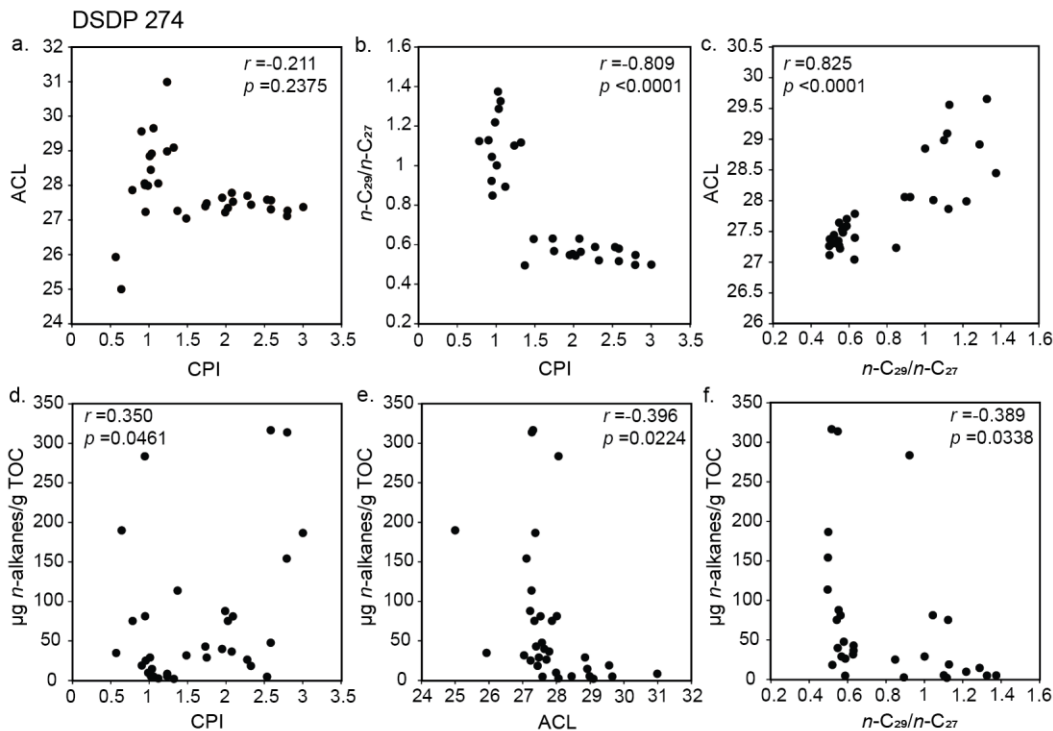
405

406

407

408

Fig. 11. Stratigraphic column from DSDP 274 with the stratigraphic positions of representative GC-FID-chromatograms of samples. Filled circles above peaks indicate n-alkanes, with the $n-C_{27}$ and $n-C_{29}$ labelled. Facies are described in table 1. UCM: unresolved complex mixture.



409

410

411

412

413

Fig. 12. Scatter plots of samples from DSDP 274; a) CPI and ACL; b) CPI and $n\text{-C}_{29}/n\text{-C}_{27}$; c) $n\text{-C}_{29}/n\text{-C}_{27}$ and ACL; d) CPI and the total abundance of n -alkanes ($\mu\text{g } n\text{-alkanes/g TOC}$); e) ACL and the total abundance of n -alkanes ($\mu\text{g } n\text{-alkanes/g TOC}$) and f) $n\text{-C}_{29}/n\text{-C}_{27}$ and the total abundance of n -alkanes ($\mu\text{g } n\text{-alkanes/g TOC}$).

414 **4 Discussion**

415 *4.1 Potential sources of lipid biomarkers in Cenozoic Antarctic sediments*

416 *4.1.1 Contemporaneous organic matter*

417 Plants and microorganisms living contemporaneously with the accumulation of sediment
 418 would have been a major contributing source for n -alkanes and hopanes with $\beta\beta$ stereochemistry at
 419 the sites studied. Macro- and microfossils from sediment cores, onland outcrops and glacial erratics
 420 indicate that the Ross Sea region of Antarctica was vegetated until at least the Mid-Miocene Climate
 421 Transition (MMCT) ~ 14 Ma (e.g. Kemp, 1975; Mildenhall, 1989; Askin, 2000; Askin and Raine,
 422 2000; Lewis et al., 2008; Warny et al., 2009; Lewis and Ashworth, 2016). Paleocene and Early
 423 Eocene sediment from cores offshore Wilkes Land indicate a highly diverse, near tropical flora
 424 occupied coastal regions, with temperate rain forest inland and at higher elevations (Pross et al.,
 425 2012). Following a prolonged period of global cooling, sediments from the Ross Sea region indicate
 426 that by the Mid-Late Eocene, vegetation was largely represented by a less diverse, cool, temperate
 427 flora dominated by *Nothofagus*-podocarpaceous conifer-*proteaceae* (Askin, 2000; Francis, 2000; Pole
 428 et al., 2000).

429 The Oligocene and early Miocene was marked by declining vegetation diversity and the
430 development of a sparse, shrubby tundra, dominated by stunted *Nothofagus* (Kemp, 1975; Kemp and
431 Barrett, 1975; Askin and Raine, 2000; Prebble et al., 2006a). The Mid-Miocene Climate Optimum
432 (MMCO) (~17-15 Ma), saw an increase in the abundance of pollen transported offshore indicating a
433 proliferation of woody vegetation and a possible return to more tree-like forms (Warny et al., 2009;
434 Feakins et al., 2012). This short-lived warming was followed by the MMCT, a major cooling step in
435 the Cenozoic (Shackleton and Kennett, 1975; Flower and Kennett, 1994; Lewis et al. 2007). The
436 vegetation history of Antarctica following the MMCT has been debated, with different schools of
437 thought suggesting that demise of higher plants occurred either at the MMCT (Sugden et al., 1993;
438 Marchant et al., 1996; Lewis et al., 2008) or the Pliocene (Harwood et al. 1983; Webb et al. 1984;
439 Fielding et al., 2012). The Pliocene ages are controversial and rely on sparse diatoms present in tills of
440 the Meyer Desert Formation, preserved in the upper Beardmore Glacier (Barrett, 2013).

441 *4.1.2 Reworked lipid biomarkers from older sediments*

442 Lipid biomarkers could also be sourced from the erosion and redeposition of older sediments.
443 Two main sources are considered here; reworked Cenozoic *n*-alkanes, and reworked Permian-Jurassic
444 biomarkers sourced from the Beacon Super Group and Ferrar Group. The presence of Cretaceous
445 dinoflagellate cysts in samples of the McMurdo erratics suggests the possibility for a contribution
446 from rocks of this age now either eroded or buried, but as these occurrences are extremely rare this
447 potential contribution is considered very minor (Askin, 2000). Surface sediment from the Eastern
448 Ross Sea does contain a significant component of Late Cretaceous palynomorphs, but the location of
449 DSDP Site 270 in the central Ross Sea does not (Truswell and Drewry, 1984). Oligocene/Late
450 Miocene sediments in this core are also barren of pollen from this time period (Kemp, 1975; Duncan,
451 2017).

452 Microfossil work on Oligocene and Miocene sediments in continental margin drillcores
453 frequently indicate the presence of older Cenozoic microfossils, likely eroded from older sedimentary
454 basin infill. In particular, Eocene aged dinoflagellate cysts of the ‘Transantarctic flora’ are used to
455 infer reworking of Eocene material into younger sediments (e.g. Kemp, 1975; Askin and Raine, 2000;
456 Prebble et al., 2006a). Limited burial of Cenozoic sediments means that Paleogene forms reworked
457 into younger sediments are still light in colour and display similar autofluorescence (e.g. Askin and
458 Raine, 2000; Prebble et al., 2006a). Here, *n*-alkanes extracted from the fossiliferous McMurdo erratics
459 serve as an indication of typical Mid-Late Eocene distributions of these compounds (Section 4.2.1).

460 The Beacon Supergroup extends throughout the TAM and is a key source of sediment to the
461 sedimentary basins of the Ross Sea (e.g. Talarico et al., 2000; Smellie, 2001; Sandroni and Talarico,
462 2004; Sandroni and Talarico, 2011). Many of the fossil assemblages from the Beacon Supergroup
463 come from widespread Permian and Triassic sediments, and indicate a cool, humid Mid-Late Permian

464 climate with vegetation dominated by *Glossopteris* and *Gangamopteris* (Cúneo et al., 1993; Francis et
465 al., 1994; Collinson, 1997). By the Mid-Triassic, a more diverse flora dominated by *Dicroidium*
466 indicates a shift to warmer ‘greenhouse’ conditions (Collinson, 1997; Cúneo et al., 2003). The Beacon
467 Supergroup outcropping in the TAM has undergone widespread intrusion and thermal alteration, with
468 altered palynomorphs in continental margin cores likely reflecting a TAM source, whilst less altered
469 specimens must have been transported from less extensively intruded sediments cratonwards of the
470 TAM (Askin, 1998; Askin and Raine, 2000). Fossiliferous sedimentary interbeds of the Jurassic
471 Ferrar group are also known to contribute reworked palynomorphs to offshore sediments, albeit with
472 much rarer occurrences than those sourced from the Beacon Supergroup (Askin and Raine, 2000). *n*-
473 Alkanes have previously been analysed from Beacon sediments, silicified wood and coal at the Allan
474 Hills and Ferrar Group sediments from Carapace Nunatak in Southern Victoria Land (Matsumoto et
475 al., 1986). *n*-Alkanes ranging from *n*-C₁₂ to *n*-C₃₀ displayed a CPI varying from 0.91-1.4. Short chain
476 *n*-alkanes (< *n*-C₂₀) were typically more abundant than long chain lengths (Matsumoto et al., 1986). A
477 chromatogram from Matsumoto et al. (1986) indicates that UCMs are also present in these samples,
478 centred at *n*-C₁₈ and *n*-C₁₉. Hopanes in these Beacon sediments were typically dominated by αβ and
479 βα configurations indicating maturation of the sediments and alteration of hopanes from their
480 biologically synthesized precursors (Matsumoto et al., 1987). Variable thermal maturation of the
481 Beacon sediments in this region is suggested by two samples containing small quantities of ββ
482 hopanes (Matsumoto et al., 1987)

483 Distributions of *n*-alkanes, kerogen and palynomorphs in surface and Quaternary sediments
484 from the Ross Sea, and soils from the Dry Valleys, suggest the potential for recycling of *n*-alkanes
485 from both Cenozoic and pre-Cenozoic sources is occurring via modern depositional processes. In the
486 Ross Sea, *n*-Alkanes appear in low abundances with short chained *n*-alkanes attributed to a mixture of
487 primary and recycled material derived from marine organisms, while long chained *n*-alkanes are
488 suggested to be higher plant material either from long-range aeolian transport or reworked from pre-
489 Quaternary sediments (Kvenvolden et al., 1987; Venkatesan, 1988). A recycled source for *n*-alkanes
490 is supported by the presence of hopanes of variable maturities (ββ, βα and αβ), and kerogen and
491 pollen extensively reworked from Paleogene or pre Cenozoic sediment (Sackett et al., 1974; Truswell
492 and Drewry, 1984, Kvenvolden et al., 1987). The most abundant *n*-alkanes in soils from the Dry
493 Valleys are usually *n*-C₂₃, *n*-C₂₅, or *n*-C₂₇ (Matsumoto et al., 1990a; Matsumoto et al., 2010; Hart et
494 al., 2011). *n*-Alkanes are attributed to a mixed source input, predominantly derived from endolithic
495 microorganisms and glacially eroded ancient plant and microorganism debris, sourced from earlier
496 Cenozoic sediments and the Beacon Sandstone (Matsumoto et al., 1990a; Matsumoto et al., 2010).
497 This is supported by the presence of mature (βα and αβ) isomers of hopanes, likely sourced from
498 Beacon sediments (Matsumoto et al., 1990b) Aeolian transport as a main source for the *n*-alkanes in
499 these samples is considered unlikely, as aerosol samples near Antarctica record *n*-alkane distributions

500 with high ACLs and a dominant n -C₃₁, potentially as a result of large scale meridional air mass
501 circulation transporting n -alkanes from the tropics to high latitudes (Bendle et al., 2007).

502 4.1.3 *In situ* degradation of n -alkanes

503 In Antarctica and the Sub-Antarctic, hydrocarbon contamination experiments indicate that
504 hydrocarbon degrading microbes are present in soils (Aislabie et al., 1998; Bej et al., 2000; Coulon et
505 al., 2005). Longer chain length n -alkanes were found to be more resistant to microbial degradation,
506 and rates of degradation increase with increasing temperature (Coulon et al., 2005). n -Alkane
507 distributions in the studied samples are not considered the result of *in situ* thermal maturation, or
508 migration of hydrocarbons into the sediments. The sediment sampled in this study comes from near
509 surface sediment in the case of Mt Boreas, or drill cores where the deepest samples come from 385
510 mbsf in DSDP 270. None of the studied cores contained hydrocarbon residues, and heat flow
511 measurements from CRP-2/2A and other cores in the region (CRP 3, ANDRILL 1B, ANDRILL 2A)
512 range from 24-76.7 °C/km (Bücker et al., 2000; Bücker et al., 2001; Morin et al., 2010; Schröder et
513 al., 2011). Basin modelling from the central and western Ross Sea shows that while the generation of
514 hydrocarbons is possible in the deeply buried sediments of the basins, expulsion and migration of
515 hydrocarbons from potential source rocks is very unlikely (Strogen and Bland, 2011).

516 4.2 n -Alkane distributions across sample sites

517 4.2.1 *McMurdo* erratics

518 The *McMurdo* erratics provide examples of mid-late Eocene n -alkane distributions, when
519 Antarctic vegetation was more diverse than in the Oligocene and Miocene, and the climate was
520 warmer and wetter (Askin, 2000; Francis, 2000; Pole et al., 2000). All of the samples except for
521 MTD95 contain a terrestrial palynomorph assemblage, with E215 and E219 also including leaves and
522 in E219, wood macrofossils (Harwood and Levy, 2000). However, these erratics do also contain a
523 minor component of reworked material sourced from the Beacon Supergroup (Askin, 2000). Despite
524 this, the occurrence of macro-fossils and dominantly Eocene-aged assemblages of palynomorphs
525 suggest that the n -alkanes in these samples are principally from contemporaneously-sourced organic
526 matter. The key difference in the n -alkane distributions of the *McMurdo* erratics compared to
527 Oligocene and Miocene samples from the other studied sites is the prominence of the n -C₂₉ as
528 opposed to the n -C₂₇ (Supplementary table 1, Fig.3). We suggest the shift from a dominant n -C₂₉ to n -
529 C₂₇ in the Ross Sea region is due to a combination of climate cooling as the Antarctic ice sheets
530 developed, and a shift in plant community to a flora dominated by a low diversity tundra of
531 *Nothofagus*, *podocarpidites* and bryophytes (Askin, 2000; Askin and Raine, 2000; Prebble et al.,
532 2006a; Lewis et al., 2008).

533 4.2.2 Mt Boreas

534 The presence of macro and microfossils of bryophytes at Mt Boreas is represented by the
535 prominence of $n\text{-C}_{23}$ and $n\text{-C}_{25}$ in the n -alkane distributions from this site (Fig. 4) (Lewis et al., 2008).
536 The $n\text{-C}_{27}$ homolog is also particularly abundant and is likely sourced from shrubs and trees such as
537 *Nothofagidites lachlaniae* in the lake catchment (Lewis et al., 2008). A correlation between increasing
538 $n\text{-C}_{29}$ and decreasing CPI could be the result of either: 1) microbial degradation lowering CPI and
539 preferentially degrading the shorter chain $n\text{-C}_{27}$; or 2) incorporation of recycled material, likely from
540 weathered, thermally-degraded Beacon Supergroup, and older Cenozoic sediments in the catchment.
541 This is supported by the presence of thermally matured hopanes in sample ALS-05 21O, which is
542 from the base of the lacustrine section, just above a glacial till containing clasts of Beacon Supergroup
543 (Lewis et al., 2008). Other samples in which hopanes were investigated were dominated by $\beta\beta$
544 hopanes, supporting an interpretation that much of the biomarkers in the rest of the lacustrine
545 sediments are contemporaneously sourced. Lacustrine depositional environments (Facies 1) have
546 higher average CPIs and lower average $n\text{-C}_{29}/n\text{-C}_{27}$ values than fluvial samples (Facies 2) (Fig. 6).
547 Fluvial environments can be erosive settings as coarser sediments require greater water velocity for
548 suspension and movement (Miller et al., 1977), suggesting a fluvially influenced environment is more
549 likely to rework n -alkanes. In the lacustrine setting, high CPI, low ACL and $n\text{-C}_{29}/n\text{-C}_{27}$ in particular
550 occur directly below, and almost directly above the moss peat (Fig. 4). n -alkane distributions are
551 likely sampling the aquatic plants and mosses deposited during a shallow water phase of the lake.
552 Samples from beds representing a deeper water phase of the lake (Lewis et al., 2008) are marked by a
553 similar average CPI and $n\text{-C}_{29}/n\text{-C}_{27}$ as the laminated silts, but a higher ACL, reflecting an increased
554 input of emergent and terrestrial plant matter from the surrounding catchment.

555 4.2.3 CRP 2/2A

556 In CRP 2/2A, n -alkane distributions typically show the $n\text{-C}_{27}$ as the dominant homolog,
557 although $n\text{-C}_{23}$, $n\text{-C}_{25}$ and $n\text{-C}_{29}$ were also commonly abundant. The prominence of these n -alkane
558 homologs is in line with palynomorph evidence which suggests input from trees, shrubs and
559 bryophytes (Prebble et al., 2006a). Fluctuating abundances of reworked palynomorphs (thermally
560 altered, poorly preserved or of a known older range) often coincide with larger abundances of Eocene
561 Transantarctic flora dinoflagellates (Prebble et al., 2006a). This indicates reworked samples were
562 sourced from both Permian/Triassic Beacon sediments and earlier Cenozoic sediments. The
563 correlations between low CPI, and high ACL and $n\text{-C}_{29}/n\text{-C}_{27}$ (Fig. 8) can be explained by a mixed
564 source input of n -alkanes, from contemporaneous material, early Cenozoic sediments, and both
565 altered and unaltered areas of the Beacon Supergroup. This is supported by the presence of both
566 biologically synthesized and thermally matured hopane configurations. While a contribution from
567 more recent recycled material (i.e Early Oligocene n -alkanes) cannot be ruled out, Prebble et al.

568 (2006b) found little evidence for reworking between Early and Late Oligocene sequences. UCMs in
569 these samples typically underlie the lower chain lengths, and may be the result of post-depositional
570 microbial alteration, or could be inherited from the Beacon Supergroup (Matsumoto et al., 1986).
571 Facies groupings reflect depositional environments which are predominantly influenced by the
572 proximity of glaciers near the site. More ice-distal, marine facies (7 and 8) have on average high CPIs,
573 low ACL and low $n\text{-C}_{29}/n\text{-C}_{27}$ (Fig. 6), while samples from ice-proximal or subglacial settings tend to
574 show the opposite trends. This suggests that low-energy, more ice-distal marine environments are
575 more likely to contain well-preserved n -alkane distributions reflecting contemporaneously sourced n -
576 alkanes, whilst more ice-proximal and subglacial environments have a higher likelihood of containing
577 reworked n -alkanes.

578 4.2.4 DSDP 270

579 n -Alkane distributions from DSDP 270 are typically bi-modal suggesting two primary sources
580 for n -alkanes in this drill core (Fig. 9). Algae and bacteria the likely source for the shorter chain
581 lengths, with terrestrial higher plants contributing to longer chain lengths (section 2.5). The presence
582 of a contemporaneous pollen assemblage with almost no reworked contribution indicates the long
583 chained n -alkanes predominantly reflect contemporary onshore vegetation. This is shown in the CPI
584 values that vary less than the other sites sampled and all sit above 2.4 (Fig. 6), and the predominance
585 of hopanes in $\beta\beta$ configurations. Facies representing more ice-proximal settings (facies 3 and 4) show
586 the lowest average CPIs suggesting that these settings are likely to contain more degraded n -alkane
587 distributions, whether as the result of post-depositional processes or some sediment recycling due to
588 glacial erosion and redeposition (Fig. 6).

589 4.2.5 DSDP 274

590 n -Alkane distributions in DSDP 274 are separated into two distinct groups, above and below
591 an unconformity/condensed section at 113.6 mbsf (Figs. 6 and 11). Samples taken from below 113.6
592 mbsf show bi-modal distributions in chromatograms suggesting a mixed contribution from both algae
593 and bacteria, and terrestrial plants. Other than the uppermost 2 samples from this section of the core,
594 all samples are considered to be part of facies 10, which was deposited with a high terrigenous and
595 biogenic sedimentation rate, under a regime of weak bottom currents (Fig. 2) (Frakes, 1975;
596 Whittaker and Müller, 2006). Reworked palynomorphs are present in this section (Kemp, 1975),
597 which, coupled with variable CPI and UCMs suggest that some contribution of reworked n -alkanes is
598 likely. However, the generally high CPI, dominance of the $n\text{-C}_{27}$ and lack of variation in ACL and n -
599 $\text{C}_{29}/n\text{-C}_{27}$ suggests that much of the n -alkanes present reflect comparatively more contemporaneous
600 input than the overlying interval, or at least material recycled from the Oligocene or younger.

601 Above the unconformity or condensed section at 113.6 mbsf, the sedimentation rate slows and
602 manganese nodules provide evidence for winnowing by a strong bottom current regime. This interval
603 is also associated with an increase in coarse sediment which could result from ice rafting (Frakes,
604 1975; Whittaker and Müller, 2006) or winnowing of the fine fraction due to intensification of bottom
605 currents. These sediments date to the Late Miocene, and Antarctic glacial expansion at this time could
606 explain the increase in ice rafting or bottom water current intensity (McKay et al., 2009; Herbert et al.,
607 2016). Sediments from this part of the core are also include and post-date the MMCT when it has
608 been debated that higher plants became extinct on Antarctica (Sugden et al., 1993; Marchant et al.,
609 1996; Lewis et al., 2008). This indicates that *n*-alkanes from this section of the core may
610 predominantly be derived from older sediments, an interpretation supported by a hopane distribution
611 dominated by thermally matured configurations. Low CPIs, high $n\text{-C}_{29}/n\text{-C}_{27}$, often large and
612 dominant UCMs and low sedimentation rates suggest that *n*-alkanes in these samples have also been
613 extensively degraded, likely by microbial activity as sediments are winnowed and reworked in the
614 surface layers of the seabed.

615 5. Synthesis

616 *n*-Alkane distributions in Eocene to Miocene sediments from the Ross Sea region vary with
617 age and sample site. Between the Eocene and Oligocene, the dominant chain length recorded in
618 sediments changes from *n*-C₂₉ to *n*-C₂₇, concomitant with a significant climate cooling and a shift in
619 plant community (section 4.2.1). The dominance of the *n*-C₂₇ in sediments sourced from wide
620 catchments incorporating a cool, low diversity vegetation dominated by *Nothofagus* is in contrast to
621 lower latitudes where *n*-C₂₉ and *n*-C₃₁ are often more abundant (e.g. Poynter et al., 1989; Kawamura
622 et al., 2003; Sachse et al., 2006; Bendle et al., 2007). At least one modern species of *Nothofagus* (*N.*
623 *menziesii*) from New Zealand has been shown to produce *n*-C₂₇ as its dominant *n*-alkane (Burrington,
624 2015), while other species in New Zealand and South America are typically dominated by *n*-C₂₉ and
625 *n*-C₃₁ (Schellekens et al., 2009; Schellekens et al., 2011; Burrington, 2015). The high abundance of *n*-
626 C₂₇ in samples from Mt Boreas also containing abundant pollen from *N. lachlaniae* suggest that this
627 species was likely producing large proportions of this *n*-alkane. The prominence of the *n*-C₂₇ across
628 the Oligocene and Miocene sites of this study likely reflects both a climate adaption by plants
629 growing in the Antarctic tundra to cold temperatures, and the abundance of *Nothofagus* in the
630 catchments.

631 While the Oligocene and Miocene vegetation of Antarctica was a main source of *n*-alkanes to
632 the sample sites, reworked *n*-alkanes and hopanes from early and pre-Cenozoic sediments were also
633 evident. In particular, variables that often characterised samples with more reworked material were
634 low CPI values, but higher ACLs and $n\text{-C}_{29}/n\text{-C}_{27}$ ratios. In a sample containing material solely from
635 reworked thermally altered sections of the Beacon Supergroup, a low CPI, ACL and $n\text{-C}_{29}/n\text{-C}_{27}$

636 would be expected (Matsumoto et al., 1986). The association of low CPIs with high ACL and $n\text{-C}_{29}/n\text{-}$
637 C_{27} therefore suggests that reworked samples likely contain a mixture of n -alkanes derived from
638 thermally matured Beacon sediments, coupled with material from early Cenozoic and less altered pre-
639 Cenozoic sediments containing a higher abundance of longer chained n -alkanes such as $n\text{-C}_{29}$ and $n\text{-}$
640 C_{31} . In some instances, this distribution could also result from microbial degradation, which could
641 lower CPI, whilst also preferentially scavenging shorter chain lengths.

642 Sediments deposited by glacio-fluvial, ice-proximal glaciomarine and subglacial processes
643 are more likely to contain reworked n -alkane distributions than those from lacustrine or ice-distal
644 marine environments, although careful site specific consideration of sediment provenance must be
645 undertaken, regardless of relative proximity to glaciers or rivers. Prior to the MMCT, glaciers
646 throughout the TAM, and likely the exposed areas of the Ross Sea, were warm-based (Marchant and
647 Denton, 1996; Lewis et al., 2007). This regime would have favoured high rates of glacial erosion of
648 underlying strata, resulting in rapid remobilisation, deposition and burial of sediment in glacial
649 proximal regions (Sugden and Denton, 2004; Powell et al. 2000). These processes likely led to the
650 deposition of greater proportions of reworked n -alkanes in ice-proximal environments. Although ice-
651 distal settings also record glaciomarine processes and may be subject to reworking, they are likely a
652 more integrated record of aeolian and glacio-fluvial sediment transport offshore. However, as
653 Antarctica became progressively more arid during the Late Miocene and Pliocene, it is feasible that
654 offshore transport of contemporaneous n -alkanes via glacio-fluvial action reduced, and thus the
655 relative input of reworked n -alkanes became more prominent (e.g. at DSDP 274).

656 The varying contribution of contemporaneous and reworked biomarkers across sediments
657 sourced from different depositional environments, catchments and ages emphasizes how caution must
658 be exercised when applying biomarker-based paleoclimate proxies in glacially-influenced settings
659 (e.g. n -alkane $\delta^{13}\text{C}$ and $\delta^2\text{H}$). In particular, several aspects should be considered when determining if
660 an n -alkane distribution is a contemporaneously-sourced organic matter signature. These include the
661 values and variation of factors such as CPI and ACL, maturation indices of other biomarkers such as
662 hopanes, whether the catchment and depositional setting of a site is more likely to accumulate and
663 preserve a contemporary distribution, and assemblages of other fossil material such as palynomorphs.
664 When constructing timeseries of biomarker assemblages, it is also important to consider other aspects
665 of the depositional environment in the Ross Sea. The coastal setting of the Ross Sea could be
666 influenced by pulses of reworked material, given the potential for point source glacial meltwater
667 discharge, and large-scale meltwater discharge events (i.e. Powell and Domack, 2002; Lewis et al.,
668 2006), which may focus erosion to a certain lithological source. Input of reworked material via
669 episodic, erosive hydrological events in Paleocene-Eocene Thermal Maximum sediments from
670 Tanzania has been invoked to explain the highly variable n -alkane $\delta^{13}\text{C}$ values in these sediments
671 (Carmichael et al., 2017). Glacially-influenced environments have a high potential to erode and

672 almost instantaneously redeposit older biomarkers and pollen offshore in concentrated numbers, and
673 indeed biomarker distributions could be used as a potential tool to identify such reworking events.

674 **6 Conclusions**

675 *n*-Alkane and hopanoid distributions have been characterised in Eocene to Miocene sediments
676 from a range of depositional environments in the Ross Sea region of Antarctica. Between the Late
677 Eocene and the Oligocene, a shift in *n*-alkane dominant chain length is observed from *n*-C₂₉ to *n*-C₂₇.
678 This is inferred to be a result of both a shift in plant community, as well as a response to significant
679 climate cooling. Biomarker distributions in Oligocene and Miocene samples varyingly display a
680 contribution from both contemporaneous and reworked sources. *n*-Alkane distributions typical of a
681 reworked sample were a low CPI, and high ACL and *n*-C₂₉/*n*-C₂₇ values. Reworked samples likely
682 reflect a mixed contribution from thermally altered and less thermally altered regions of the Mesozoic
683 Beacon Super Group, coupled with material sourced from earlier Cenozoic sediments. Microbial
684 degradation during transport and post-deposition may also contribute to these distributions. Samples
685 dominated by contemporaneously-sourced organic matter display a higher CPI, and lower ACL and *n*-
686 C₂₉/*n*-C₂₇ values. These *n*-alkanes were sourced from the sparse, cold tundra which existed during this
687 time. Fluvial environments onshore, and subglacial and ice-proximal environments offshore were
688 more likely to contain reworked *n*-alkanes. Lacustrine environments onshore, and ice-distal
689 environments offshore, were more likely to contain contemporary *n*-alkanes. These findings indicate
690 the possibility of reworking should be taken into account when biomarkers are used for paleoclimate
691 studies in ice-marginal environments.

692 **7 Acknowledgments**

693 The authors are grateful for access to samples from the IODP core repository at Texas A&M
694 University for DSDP Sites 270 and 274. This study was funded via an Antarctica New Zealand Sir
695 Robin Irvine PhD Scholarship and Scientific Committee of Antarctic Research Fellowship awarded to
696 Bella Duncan, with additional funding from a Royal Society of New Zealand Rutherford Discovery
697 Fellowship awarded to Rob McKay (RDF-13-VUW-003) and New Zealand Ministry of Business
698 Innovation and Employment Contract C05X1001. Field activities were supported by Antarctica New
699 Zealand. The authors are grateful for support from IODP and support in kind from the University of
700 Birmingham. The authors thank two anonymous reviewers for their constructive comments.

701 **Data Availability**

702 Data associated with this study can be found in the supplementary tables.

703 **References**

- 704 Aislabie, J., McLeod, M., Fraser, R., 1998. Potential for biodegradation of hydrocarbons in soil from
705 the Ross Dependency, Antarctica. *Applied Microbiology and Biotechnology* 49, 210-214.
- 706 Allibone, A.H., Cox, S.C., Graham, I.J., Smillie, R.W., Johnstone, R.D., Ellery, S.G., Palmer, K.,
707 1993. Granitoids of the Dry Valleys area, southern Victoria Land, Antarctica: plutons, field
708 relationships, and isotopic dating. *New Zealand journal of geology and geophysics* 36, 281-297.
- 709 Allibone, A.H., Cox, S.C., Smillie, R.W., 1993. Granitoids of the Dry Valleys area, southern Victoria
710 Land: geochemistry and evolution along the early Paleozoic Antarctic Craton margin. *New
711 Zealand journal of geology and geophysics* 36, 299-316.
- 712 Askin, R.A., 1998. Palynological investigations of Mount Feather Sirius Group samples: recycled
713 Triassic assemblages, In: Wilson, G.S., Barron, J. (Eds.), *Mount Feather Sirius Group Core
714 Workshop and Collaborative Sample Analysis*. Byrd Polar Research Center Report No. 14.
715 Byrd Polar Research Center, The Ohio State University, Columbus, Ohio, pp. 59-65.
- 716 Askin, R.A., 2000. Spores and pollen from the McMurdo Sound erratics, Antarctica. In: Stilwel, J.D.,
717 Feldman, R.M. (Eds.), *Paleobiology and Paleoenvironments of Eocene Rocks: McMurdo
718 Sound, East Antarctica*. American Geophysical Union, Washington, D.C., pp. 161-181.
- 719 Askin, R.A., Raine, J.I., 2000. Oligocene and Early Miocene terrestrial palynology of the Cape
720 Roberts Drillhole CRP-2/2A, Victoria Land Basin, Antarctica. *Terra Antarctica* 7, 493-501.
- 721 Barrett, P.J., 1981. History of the Ross Sea region during the deposition of the Beacon Supergroup
722 400-180 million years ago. *Journal of the Royal Society of New Zealand* 11, 447-458.
- 723 Barrett, P.J., Elliot, D.H., Lindsay, J.F., 1986. The Beacon Supergroup (Devonian- Triassic) and
724 Ferrar Group (Jurassic) in the Beardmore Glacier Area, Antarctica. In: Turner, M.D.,
725 Spletstoesser J.E. (Eds.), *Geology of the central Transantarctic Mountains*. American
726 Geophysical Union, Washington, D.C., pp. 339-428.
- 727 Barrett, P.J. (Ed.). 1989. *Antarctic Cenozoic history from the CIROS-1 drillhole, McMurdo Sound*.
728 DSIR Publishing, Wellington, New Zealand.
- 729 Barrett, P.J., 2013. Resolving views on Antarctic Neogene glacial history—the Sirius debate. *Earth and
730 Environmental Science Transactions of the Royal Society of Edinburgh* 104, 31-53.
- 731 Bej, A.K., Saul, D., Aislabie, J., 2000. Cold-tolerant alkane-degrading *Rhodococcus* species from
732 Antarctica. *Polar Biology* 23, 100-105.
- 733 Bendle, J., Kawamura, K., Yamazaki, K., Niwai, T., 2007. Latitudinal distribution of terrestrial lipid
734 biomarkers and n-alkane compound-specific stable carbon isotope ratios in the atmosphere over
735 the western Pacific and Southern Ocean. *Geochimica et Cosmochimica Acta* 71(24), 5934-
736 5955.
- 737 Bijl, P.K., Bendle, J.A., Bohaty, S.M., Pross, J., Schouten, S., Tauxe, L., Stickley, C.E., McKay, R.M.,
738 Röhl, U., Olney, M., Sluijs, A., Escutia, C., Brinkhuis, H., Expedition 318 Scientists, 2013.

739 Eocene cooling linked to early flow across the Tasmanian Gateway. *Proceedings of the*
740 *National Academy of Sciences* 110, 9645-9650.

741 Bray, E.E., Evans, E.D., 1961. Distribution of n-paraffins as a clue to recognition of source
742 beds. *Geochimica et Cosmochimica Acta* 22, 2-15.

743 Bücker, C.J., Wonik, T., Jarrard, R., 2000. The temperature and salinity profile in CRP-2/2A, Victoria
744 Land Basin, Antarctica. *Terra Antarctica* 7, 255-259.

745 Bücker, C., Jarrard, R.D., Wonik, T., 2001. Downhole temperature, radiogenic heat production, and
746 heat flow from the CRP-3 drillhole, Victoria Land Basin, Antarctica. *Terra Antarctica* 8, 151-
747 160.

748 Burrington, P., 2015. How to be a Prehistoric Weatherman: Using n-alkanes as a Proxy for Holocene
749 Climate and Hydrology, Southwest South Island, New Zealand (Unpublished Masters Thesis).
750 University of Otago, New Zealand.

751 Bush, R.T., McInerney, F.A., 2013. Leaf wax n-alkane distributions in and across modern plants:
752 implications for paleoecology and chemotaxonomy. *Geochimica et Cosmochimica Acta* 117,
753 161-179.

754 Bush, R.T., McInerney, F.A., 2015. Influence of temperature and C₄ abundance on n-alkane chain
755 length distributions across the central USA. *Organic Geochemistry* 79, 65-73.

756 Calvo, E., Pelejero, C., Logan, G.A., De Deckker, P., 2004. Dust-induced changes in phytoplankton
757 composition in the Tasman Sea during the last four glacial cycles. *Paleoceanography* 19.

758 Cape Roberts Science Team, 1999. Studies from the Cape Roberts Project, Ross Sea Antarctica,
759 Initial report on CRP-2/2A. *Terra Antarctica* 6(1), 1-173.

760 Carmichael, M. J., Inglis, G. N., Badger, M. P., Naafs, B. D. A., Behrooz, L., Remmelzwaal, S.,
761 Monteiro, F. M., Rohrsen, M., Farnsworth, A., Buss, H. L., Dickson, A. J., Valdes, P. J., Lunt,
762 D. J., Pancost, R. D., 2017. Hydrological and associated biogeochemical consequences of rapid
763 global warming during the Paleocene-Eocene Thermal Maximum. *Global and Planetary*
764 *Change* 157, 114-138.

765 Clark Jr, R.C., Blumer, M., 1967. Distribution of n-paraffins in marine organisms and
766 sediment. *Limnology and Oceanography* 12, 79-87.

767 Collinson, J.W., 1997. Paleoclimate of Permo-Triassic Antarctica. *International Symposium on*
768 *Antarctic Earth Sciences* 7, 1029-1034.

769 Cooper, A.K., Davey, F.J., Behrendt, J.C., 1987. Seismic stratigraphy and structure of the Victoria
770 Land basin, western Ross Sea, Antarctica. In: Cooper, A.K., Davey, F.J. (Eds.), *The Antarctic*
771 *Continental Margin: Geology and Geophysics of the Western Ross Sea*. Circumpacific Council
772 for Energy and Mineral Resources, Houston, T.X., pp. 27-65.

773 Coulon, F., Pelletier, E., Gourhant, L., Delille, D., 2005. Effects of nutrient and temperature on
774 degradation of petroleum hydrocarbons in contaminated sub-Antarctic soil. *Chemosphere* 58,
775 1439-1448.

776 Cranwell, P.A., Eglinton, G., Robinson, N., 1987. Lipids of aquatic organisms as potential
777 contributors to lacustrine sediments—II. *Organic Geochemistry* 11, 513-527.

778 Cúneo, N.R., Isbell, J., Taylor, E.L., Taylor, T.N., 1993. The Glossopteris flora from Antarctica:
779 taphonomy and paleoecology. *Comptes Rendus XII ICC-P 2*, 13-40.

780 Cúneo, N.R., Taylor, E.L., Taylor, T.N., Krings, M., 2003. In situ fossil forest from the upper
781 Fremouw Formation (Triassic) of Antarctica: paleoenvironmental setting and paleoclimate
782 analysis. *Palaeogeography, Palaeoclimatology, Palaeoecology* 197, 239-261.

783 Decesari, R.C., Sorlien, C.C., Luyendyk, B.P., Wilson, D.S., Bartek, L.R., Diebold, J., Hopkins, S.E.,
784 2007. Regional seismic stratigraphic correlations of the Ross Sea: implications for the tectonic
785 history of the West Antarctic Rift System. In: Cooper, A.K., Raymond, C.R., 10th ISAES
786 Editorial Team (Eds.), *Antarctica: A Keystone in a Changing World- Online Proceedings of the*
787 *10th ISAES, 2007-1047, USGS Open-File Report, Short Research Paper 052*, 4p.

788 De Santis, L., Anderson, J.B., Brancolini, G., Zayatz, I., 1995. Seismic record of late Oligocene
789 through Miocene glaciation on the central and eastern continental shelf of the Ross Sea. In:
790 Cooper, A.K., Barker, P.F., Brancolini, G. (Eds.), *Geology and Seismic Stratigraphy of the*
791 *Antarctic Margin. American Geophysical Union, Washington, D.C.*, pp. 235-260.

792 Dodd, R.S., Rafii, Z.A., Power, A.B., 1998. Ecotypic adaptation in *Austrocedrus chilensis* in cuticular
793 hydrocarbon composition. *New Phytologist* 138, 699-708.

794 Dodd, R.S., Afzal-Rafii, Z., 2000. Habitat-related adaptive properties of plant cuticular
795 lipids. *Evolution* 54, 1438-1444.

796 Duncan, B.J., 2017. Cenozoic Antarctic climate evolution based on molecular and isotopic biomarker
797 reconstructions from geological archives in the Ross Sea region (Unpublished PhD Thesis).
798 Victoria University of Wellington, New Zealand.

799 Eglinton, G., Hamilton, R.J., 1963. The distribution of alkanes. *Chemical plant taxonomy* 187, 217.

800 Farrimond, P., Taylor, A., Telnæs, N., 1998. Biomarker maturity parameters: the role of generation
801 and thermal degradation. *Organic Geochemistry* 29, 1181-1197.

802 Feakins, S.J., Warny, S., Lee, J.E., 2012. Hydrologic cycling over Antarctica during the middle
803 Miocene warming. *Nature Geoscience* 5, 557-560.

804 Feakins, S.J., Warny, S., DeConto, R.M., 2014. Snapshot of cooling and drying before onset of
805 Antarctic Glaciation. *Earth and Planetary Science Letters* 404, 154-166.

806 Feakins, S.J., Peters, T., Wu, M.S., Shenkin, A., Salinas, N., Girardin, C.A., Bentley, L.P., Blonder,
807 B., Enquist, B.J., Martin, R.E., Asner, G.P., Asner, G.P., 2016. Production of leaf wax n-
808 alkanes across a tropical forest elevation transect. *Organic Geochemistry* 100, 89-100.

809 Ficken, K.J., Li, B., Swain, D.L., Eglinton, G., 2000. An n-alkane proxy for the sedimentary input of
810 submerged/floating freshwater aquatic macrophytes. *Organic Geochemistry* 31, 745-749.

811 Fielding, C.R., Naish, T.R., Woolfe, K., Lavelle, M., 2000. Facies analysis and sequence stratigraphy
812 of CRP-2/2A, Victoria Land Basin, Antarctica. *Terra Antarctica* 7, 323-338.

813 Fielding, C.R., Henrys, S.A., Wilson, T.J., 2006. Rift history of the western Victoria Land Basin: a
814 new perspective based on integration of cores with seismic reflection data. In D.K. Fütterer, D.
815 Damaske, G. Kleinschmidt, H. Miller & F. Tessensohn (Eds.), *Antarctica* (pp. 309-318). Berlin
816 Heidelberg: Springer.

817 Fielding, C.R., Harwood, D.M., Winter, D.M., Francis, J.E., 2012. Neogene stratigraphy of Taylor
818 Valley, Transantarctic Mountains, Antarctica: evidence for climate dynamism and a vegetated
819 early Pliocene coastline of McMurdo Sound. *Global and Planetary Change* 96-97, 97-104.

820 Fitzgerald, P.G., 1994. Thermochronologic constraints on post-Paleozoic tectonic evolution of the
821 central Transantarctic Mountains, Antarctica. *Tectonics* 13, 818-836.

822 Flower, B.P., Kennett, J.P., 1994. The middle Miocene climatic transition: East Antarctic ice sheet
823 development, deep ocean circulation and global carbon cycling. *Palaeogeography,*
824 *palaeoclimatology, palaeoecology* 108, 537-555.

825 Frakes, L.A., 1975. Paleoclimatic significance of some sedimentary components at Site 274. *Initial*
826 *Reports of the Deep Sea Drilling Project* 28, 785-787.

827 Francis, J.E., Woolfe, K.J., Arnott, M.J., Barrett, P.J., 1994. Permian climates of the southern margins
828 of Pangea: evidence from fossil wood in Antarctica. *Pangea: Global Environments and*
829 *Resources- Memoir* 17, 275-282.

830 Francis, J.E., Hill, R.S., 1996. Fossil plants from the Pliocene Sirius Group, Transantarctic Mountains:
831 Evidence for climate from growth rings and fossil leaves. *Palaios* 11, 389-396.

832 Francis, J.E., 2000. Fossil Wood from Eocene High Latitude Forests: McMurdo Sound, Antarctica. In:
833 Stilwel, J.D., Feldman, R.M. (Eds.), *Paleobiology and Paleoenvironments of Eocene Rocks:*
834 *McMurdo Sound, East Antarctica.* American Geophysical Union, Washington, D.C., pp. 253-
835 260.

836 Gagosian, R.B., Peltzer, E.T., 1986. The importance of atmospheric input of terrestrial organic
837 material to deep sea sediments. *Organic Geochemistry* 10, 661-669.

838 Goodge, J.W., Myrow, P., Williams, I.S., Bowring, S.A., 2002. Age and provenance of the
839 Beardmore Group, Antarctica: constraints on Rodinia supercontinent breakup. *The Journal of*
840 *geology* 110, 393-406.

841 Gough, M.A., Rowland, S.J., 1990. Characterization of unresolved complex mixtures of hydrocarbons
842 in petroleum. *Nature* 344, 648-650.

843 Gough, M.A., Rhead, M.M., Rowland, S.J., 1992. Biodegradation studies of unresolved complex
844 mixtures of hydrocarbons: model UCM hydrocarbons and the aliphatic UCM. *Organic*
845 *Geochemistry* 18, 17-22.

846 Grimalt, J., Albaigés, J., Al-Saad, H.T., Douabul, A.A.Z., 1985. n-Alkane distributions in surface
847 sediments from the Arabian Gulf. *Naturwissenschaften* 72, 35-37.

848 Grimalt, J., Albaigés, J., 1987. Sources and occurrence of C₁₂-C₂₂ n-alkane distributions with even
849 carbon-number preference in sedimentary environments. *Geochimica et Cosmochimica Acta*
850 51, 1379-1384.

851 Hambrey, M.J., Barrett, P.J. 1993. Cenozoic sedimentary and climatic record, Ross Sea region,
852 Antarctica. In: Kennett, J.P., Warnke, D.A. (Eds.) *The Antarctic Paleoenvironment: A*
853 *Perspective on Global Change: Part Two*, American Geophysical Union, Washington, D.C., pp.
854 91-124.

855 Han, J., Calvin, M., 1969. Hydrocarbon distribution of algae and bacteria, and microbiological
856 activity in sediments. *Proceedings of the National Academy of Sciences* 64, 436-443.

857 Hart, K.M., Szpak, M.T., Mahaney, W.C., Dohm, J.M., Jordan, S.F., Frazer, A.R., Allen, C.C.R.,
858 Kelleher, B.P., 2011. A bacterial enrichment study and overview of the extractable lipids from
859 paleosols in the Dry Valleys, Antarctica: implications for future Mars
860 reconnaissance. *Astrobiology* 11, 303-321.

861 Harwood, D.M., 1983. Diatoms from the Sirius Formation, Transantarctic Mountains. *Antarctic*
862 *Journal of the United States* 18, 98-100.

863 Harwood, D.M., Levy, R.H., 2000. The McMurdo Erratics: introduction and overview. In: Stilwel,
864 J.D., Feldman, R.M. (Eds.), *Paleobiology and Paleoenvironments of Eocene Rocks: McMurdo*
865 *Sound, East Antarctica*, American Geophysical Union, Washington, D.C., pp. 1-18.

866 Herbert, T.D., Lawrence, K.T., Tzanova, A., Peterson, L.C., Caballero-Gill, R., Kelly, C.S., 2016.
867 Late Miocene global cooling and the rise of modern ecosystems. *Nature Geoscience* 9, 843-
868 847.

869 Inglis, G. N., Naafs, B. D. A., Zheng, Y., McClymont, E. L., Evershed, R. P., Pancost, R. D., 2018.
870 Distributions of geohopanoids in peat: Implications for the use of hopanoid-based proxies in
871 natural archives. *Geochimica et Cosmochimica Acta* 224, 249-261.

872 Kawamura, K., Ishimura, Y., Yamazaki, K., 2003. Four years' observations of terrestrial lipid class
873 compounds in marine aerosols from the western North Pacific. *Global Biogeochemical*
874 *Cycles* 17, 3-1-3-19.

875 Kemp, E.M., 1975. Palynology of Leg 28 drill sites, Deep Sea Drilling Project. *Initial Reports of the*
876 *Deep Sea Drilling Project* 28, 599-623.

877 Kemp, E.M., Barrett, P. J., 1975. Antarctic glaciation and early Tertiary vegetation. *Nature* 258, 507-
878 508.

879 Kraus, C., 2016. Oligocene to early Miocene glacial marine sedimentation of the central Ross Sea, and
880 implications for the evolution of the West Antarctic Ice Sheet (Unpublished Masters Thesis).
881 Victoria University of Wellington, New Zealand.

882 Kvenvolden, K.A., Rapp, J.B., Golan-Bac, M., Hostettler, F.D., 1987. Multiple sources of alkanes in
883 Quaternary oceanic sediment of Antarctica. *Organic geochemistry* 11, 291-302.

- 884 Lehtonen, K., Ketola, M., 1993. Solvent-extractable lipids of Sphagnum, Carex, Bryales and Carex-
885 Bryales peats: content and compositional features vs peat humification. *Organic*
886 *Geochemistry* 20, 363-380.
- 887 Levy, R.H., Harwood, D.M., 2000. Tertiary marine palynomorphs from the McMurdo Sound erratics,
888 Antarctica. In Stilwel, J.D., Feldman, R.M. (Eds.), *Paleobiology and Paleoenvironments of*
889 *Eocene Rocks: McMurdo Sound, East Antarctica*, American Geophysical Union, Washington,
890 D.C., pp. 183-242.
- 891 Levy, R., Harwood, D., Florindo, F., Sangiorgi, F., Tripathi, R., von Eynatten, H., Gasson, E., Kuhn,
892 G., Tripathi, A., DeConto, R., Fielding, C., Field, B., Golledge, N., McKay, R., Naish, T., Olney,
893 M., Pollard, D., Schouten, S., Talarico, F., Warny, S., Willmott, V., Acton, G., Panter, K.,
894 Paulsen, T., Taviani, M., SMS Science Team, 2016. Antarctic ice sheet sensitivity to
895 atmospheric CO₂ variations in the early to mid-Miocene. *Proceedings of the National Academy*
896 *of Sciences* 113, 3453-3458.
- 897 Lewis, A.R., Marchant, D.R., Kowalewski, D.E., Baldwin, S.L., Webb, L.E., 2006. The age and
898 origin of the Labyrinth, western Dry Valleys, Antarctica: Evidence for extensive middle
899 Miocene subglacial floods and freshwater discharge to the Southern Ocean. *Geology* 34, 513-
900 516.
- 901 Lewis, A.R., Marchant, D.R., Ashworth, A.C., Hemming, S.R., Machlus, M.L., 2007. Major middle
902 Miocene global climate change: Evidence from East Antarctica and the Transantarctic
903 Mountains. *Geological Society of America Bulletin* 119, 1449-1461.
- 904 Lewis, A.R., Marchant, D.R., Ashworth, A.C., Hedenäs, L., Hemming, S.R., Johnson, J.V., Leng,
905 M.J., Machlus, M.L., Newton, A.E., Raine, J.I., Willenbring, J.K., Williams, M., Wolfe, A.P.,
906 2008. Mid-Miocene cooling and the extinction of tundra in continental Antarctica. *Proceedings*
907 *of the National Academy of Sciences* 105, 10676-10680.
- 908 Lewis, A.R., Ashworth, A.C., 2016. An early to middle Miocene record of ice-sheet and landscape
909 evolution from the Friis Hills, Antarctica. *Geological Society of America Bulletin* 128, 719-
910 738.
- 911 Luyendyk, B.P., Sorlien, C.C., Wilson, D.S., Bartek, L.R., Siddoway, C.S., 2001. Structural and
912 tectonic evolution of the Ross Sea rift in the Cape Colbeck region, Eastern Ross Sea,
913 Antarctica. *Tectonics* 20, 933-958.
- 914 Madureira, L.A., Piccinini, A., 1999. Lipids as indicators of paleoclimatic changes, II: terrestrial
915 biomarkers. *Revista Brasileira de Oceanografia* 47, 115-125.
- 916 Marchant, D.R., Denton, G.H., 1996. Miocene and Pliocene paleoclimate of the Dry Valleys region,
917 southern Victoria Land: a geomorphological approach. *Marine Micropaleontology* 27, 253-271.
- 918 Marchant, D.R., Denton, G.H., Swisher, C.C., Potter, N., 1996. Late Cenozoic Antarctic paleoclimate
919 reconstructed from volcanic ashes in the Dry Valleys region of southern Victoria
920 Land. *Geological Society of America Bulletin* 108, 181-194.

- 921 Martin, A.P., Cooper, A.F., Dunlap, W.J., 2010. Geochronology of Mount Morning, Antarctica: two-
922 phase evolution of a long-lived trachyte-basanite-phonolite eruptive center. *Bulletin of*
923 *Volcanology* 72, 357-371.
- 924 Matsumoto, G.I., Funaki, M., Machihara, T., Watanuki, K., 1986. Alkanes and alkanolic acids in the
925 Beacon Supergroup samples from the Allan Hills and the Carapace Nunatak in
926 Antarctica. *Memoirs of National Institute of Polar Research. Special issue* 43, 149-158.
- 927 Matsumoto, G. I., Machihara, T., Suzuki, N., Funaki, M., Watanuki, K., 1987. Steranes and
928 triterpanes in the Beacon Supergroup samples from southern Victoria Land in Antarctica.
929 *Geochimica et Cosmochimica Acta* 51, 2663-2671.
- 930 Matsumoto, G.I., Akiyama, M., Watanuki, K., Torii, T., 1990a. Unusual distributions of long-chain n-
931 alkanes and n-alkenes in Antarctic soil. *Organic Geochemistry* 15, 403-412.
- 932 Matsumoto, G. I., Hirai, A., Hirota, K., Watanuki, K., 1990b. Organic geochemistry of the McMurdo
933 dry valleys soil, Antarctica. *Organic Geochemistry* 16, 781-791.
- 934 Matsumoto, G.I., Honda, E., Sonoda, K., Yamamoto, S., Takemura, T., 2010. Geochemical features
935 and sources of hydrocarbons and fatty acids in soils from the McMurdo Dry Valleys in the
936 Antarctic. *Polar Science* 4, 187-196.
- 937 McKay, R., Browne, G., Carter, L., Cowan, E., Dunbar, G., Krissek, L., Naish, T., Powell, R., Reed,
938 J., Talarico, F., Wilch, T., 2009. The stratigraphic signature of the late Cenozoic Antarctic Ice
939 Sheets in the Ross Embayment. *Geological Society of America Bulletin* 121, 1537-1561.
- 940 McKay, R., Naish, T., Carter, L., Riesselman, C., Dunbar, R., Sjunneskog, C., Winter, D., Sangiorgi,
941 F., Warren, C., Pagini, M., Schouten, S., Willmott, V., Levy, R., DeConto R., Powell, R. D.,
942 2012. Antarctic and Southern Ocean influences on Late Pliocene global cooling. *Proceedings of*
943 *the National Academy of Sciences* 109, 6423-6428.
- 944 Mackenzie, A. S., Patience, R. L., Maxwell, J. R., Vandenbroucke, M., Durand, B., 1980. Molecular
945 parameters of maturation in the Toarcian shales, Paris Basin, France—I. Changes in the
946 configurations of acyclic isoprenoid alkanes, steranes and triterpanes. *Geochimica et*
947 *Cosmochimica Acta* 44, 1709-1721.
- 948 Meyers, P.A., Ishiwatari, R., 1993. Lacustrine organic geochemistry—an overview of indicators of
949 organic matter sources and diagenesis in lake sediments. *Organic geochemistry* 20, 867-900.
- 950 Mildenhall, D.C., 1989. Terrestrial palynology. In: Barrett, P.J. (Ed.), *Antarctic Cenozoic history from*
951 *the CIROS-1 drillhole, McMurdo Sound*. DSIR Publishing, Wellington, New Zealand, pp. 119-
952 127.
- 953 Miller, M.C., McCave, I.N., Komar, P., 1977. Threshold of sediment motion under unidirectional
954 currents. *Sedimentology* 24, 507-527.
- 955 Moossen, H., Bendle, J., Seki, O., Quillmann, U., Kawamura, K., 2015. North Atlantic Holocene
956 climate evolution recorded by high-resolution terrestrial and marine biomarker
957 records. *Quaternary Science Reviews* 129, 111-127.

958 Morin, R.H., Williams, T., Henrys, S.A., Magens, D., Niessen, F., Hansaraj, D., 2010. Heat flow and
959 hydrologic characteristics at the AND-1B borehole, ANDRILL McMurdo Ice Shelf Project,
960 Antarctica. *Geosphere* 6, 370-378.

961 Naish, T.R., Barrett, P.J., Dunbar, G.B., Woolfe, K.J., Dunn, A.G., Henrys, S.A., Claps, M., Powell,
962 R.D., Fielding, C.R., 2001. Sedimentary cyclicity in CRP drillcore, Victoria Land Basin,
963 Antarctica. *Terra Antarctica* 8, 225-244.

964 Naish, T., Powell, R., Levy, R., Wilson, G., Scherer, R., Talarico, F., Krissek, L., Niessen, F.,
965 Pompilio, M., Wilson, T., Carter, L., DeConto, R., Huybers, P., McKay, R., Pollard, D., Ross,
966 J., Winter, D., Barrett, P., Browne, G., Cody, R., Cowan, E., Crampton, J., Dunbar, G., Dunbar,
967 N., Florindo, F., Gebhardt, C., Graham, I., Hannah, M., Hansaraj, D., Harwood, D., Helling, D.,
968 Henrys, S., Hinnov, L., Kuhn, G., Kyle, P., Läufer, A., Maffioli, P., Magens, D., Mandernack,
969 K., McIntosh, W., Millan, C., Morin R., Ohneiser, C., Paulsen, T., Persico, D., Raine, I., Reed,
970 J., Riesselman, C., Sagnotti, L., Schmitt, D., Sjunneskog, C., Strong, P., Taviani, M., Vogel, S.,
971 Wilch T., Williams, T., 2009. Obliquity-paced Pliocene West Antarctic ice sheet oscillation.
972 *Nature* 458, 322-328.

973 Ourisson, G., Albrecht, P., 1992. Hopanoids. 1. Geohopanoids: the most abundant natural products on
974 Earth? *Accounts of Chemical Research* 25, 398-402.

975 Peters, K. E., Moldowan, J. M., 1991. Effects of source, thermal maturity, and biodegradation on the
976 distribution and isomerization of homohopanes in petroleum. *Organic geochemistry* 17, 47-61.

977 Pole, M., Hill, B., Harwood, D., 2000. Eocene plant macrofossils from erratics, McMurdo Sound,
978 Antarctica. In: Stilwel, J.D., Feldman, R.M. (Eds.), *Paleobiology and Paleoenvironments of*
979 *Eocene Rocks: McMurdo Sound, East Antarctica*, American Geophysical Union, Washington,
980 D.C., pp. 243-251.

981 Powell, R., Krissek, L.A., Van der Meer, J., 2000. Preliminary depositional environmental analysis of
982 CRP-2/2A, Victoria Land Basin, Antarctica: palaeoglaciological and palaeoclimatic
983 inferences. *Terra Antarctica* 7, 313-322.

984 Powell, R.D., Cooper, J.M., 2002. A glacial sequence stratigraphic model for temperate, glaciated
985 continental shelves. *Geological Society, London, Special Publications* 203, 215-244.

986 Powell, R.D., Domack, E.W., 2002. Modern glacimarine environments. In: Menzies, J. (Ed.), *Modern*
987 *and Past Glacial Environments*, Butterworth-Heinemann, Boston, pp. 361-390.

988 Poynter, J.G., Farrimond, P., Robinson, N., Eglinton, G., 1989. Aeolian-derived higher plant lipids in
989 the marine sedimentary record: Links with palaeoclimate. In: Leinen, M., Sarnthein, M.,
990 (Eds.), *Paleoclimatology and paleometeorology: modern and past patterns of global*
991 *atmospheric transport*, Springer, Netherlands, pp. 435-462

992 Prebble, J.G., Raine, J.I., Barrett, P.J., Hannah, M.J., 2006a. Vegetation and climate from two
993 Oligocene glacioeustatic sedimentary cycles (31 and 24 Ma) cored by the Cape Roberts Project,

994 Victoria Land Basin, Antarctica. *Palaeogeography, Palaeoclimatology, Palaeoecology* 23, 41-
 995 57.

996 Prebble, J.G., Hannah, M.J., Barrett, P.J., 2006b. Changing Oligocene climate recorded by
 997 palynomorphs from two glacio-eustatic sedimentary cycles, Cape Roberts Project, Victoria
 998 Land Basin, Antarctica. *Palaeogeography, Palaeoclimatology, Palaeoecology* 231, 58-70.

999 Pross, J., Contreras, L., Bijl, P.K., Greenwood, D. R., Bohaty, S.M., Schouten, S., Bendle, J.A., Röhl,
 1000 U., Tauxe, L., Raine, J.I., Huck, C.E., van de Flierdt, T., Jamieson, S.S.R., Stickley, C.E., van
 1001 de Scootbrugge, B., Escutia, C., Brinkhuis, H., Integrated Ocean Drilling Program Expedition
 1002 318 Scientists, 2012. Persistent near-tropical warmth on the Antarctic continent during the early
 1003 Eocene epoch. *Nature* 488, 73-77.

1004 Rees-Owen, R.L., Gill, F.L., Newton, R.J., Ivanović, R.F., Francis, J.E., Riding, J.B., Vane, C.H., dos
 1005 Santos, R.A.L., 2018. The last forests on Antarctica: Reconstructing flora and temperature from
 1006 the Neogene Sirius Group, Transantarctic Mountains. *Organic Geochemistry*
 1007 doi.org/10.1016/j.orggeochem.2018.01.001.

1008 Ribecai, C., 2007. Early Jurassic miospores from Ferrar Group of Carapace Nunatak, South Victoria
 1009 Land, Antarctica. *Review of Palaeobotany and Palynology* 144, 3-12.

1010 Rohmer, M., Bouvier-Nave, P., Ourisson, G., 1984. Distribution of hopanoid triterpenes in
 1011 prokaryotes. *Microbiology* 130, 1137-1150.

1012 Sachse, D., Radke, J., Gleixner, G., 2006. δD values of individual n-alkanes from terrestrial plants
 1013 along a climatic gradient—Implications for the sedimentary biomarker record. *Organic*
 1014 *Geochemistry* 37, 469-483.

1015 Sackett, W.M., Poag, C.W., Eadie, B.J., 1974. Kerogen recycling in the Ross Sea,
 1016 Antarctica. *Science* 185, 1045-1047.

1017 Sandroni, S., Talarico, F., 2004. Petrography and provenance of basement clasts in CIROS-1 core,
 1018 McMurdo Sound, Antarctica. *Terra Antarctica* 11, 93-114.

1019 Sandroni, S., Talarico, F.M., 2011. The record of Miocene climatic events in AND-2A drill core
 1020 (Antarctica): Insights from provenance analyses of basement clasts. *Global and Planetary*
 1021 *Change* 75, 31-46.

1022 Schefuß, E., Ratmeyer, V., Stuut, J.B.W., Jansen, J.H.F., Sinninghe Damsté, J.S., 2003. Carbon
 1023 isotope analyses of n-alkanes in dust from the lower atmosphere over the central eastern
 1024 Atlantic. *Geochimica et Cosmochimica Acta* 67, 1757-1767.

1025 Schellekens, J., Buurman, P., Pontevedra-Pombal, X., 2009. Selecting parameters for the
 1026 environmental interpretation of peat molecular chemistry—a pyrolysis-GC/MS study. *Organic*
 1027 *Geochemistry* 40, 678-691.

1028 Schellekens, J., Buurman, P., 2011. n-Alkane distributions as palaeoclimatic proxies in ombrotrophic
 1029 peat: the role of decomposition and dominant vegetation. *Geoderma* 164, 112-121.

- 1030 Scherer, R., Hannah, M., Maffioli, P., Persico, D., Sjunneskog, C., Strong, C. P., Taviani, M., Winter,
1031 D., 2007. Palaeontologic characterisation and analysis of the AND-1B core, ANDRILL
1032 McMurdo Ice Shelf Project, Antarctica. *Terra Antarctica* 14, 223-254.
- 1033 Schröder, H., Paulsen, T., Wonik, T., 2011. Thermal properties of the AND-2A borehole in the
1034 southern Victoria Land Basin, McMurdo Sound, Antarctica. *Geosphere* 7, 1324-1330.
- 1035 Seifert, W. K., Moldowan, J. M., 1978. Applications of steranes, terpanes and monoaromatics to the
1036 maturation, migration and source of crude oils. *Geochimica et Cosmochimica Acta* 42, 77-95.
- 1037 Seifert, W. K., Moldowan, J. M., 1980. The effect of thermal stress on source-rock quality as
1038 measured by hopane stereochemistry. *Physics and Chemistry of the Earth* 12, 229-237.
- 1039 Shackleton, N.J., Kennett, J.P., 1975. Paleotemperature history of the Cenozoic and the initiation of
1040 Antarctic glaciation: oxygen and carbon isotope analyses in DSDP Sites 277, 279, and
1041 281. *Initial reports of the deep sea drilling project* 29, 743-755.
- 1042 Smellie, J.L., 2001. History of Oligocene erosion, uplift and unroofing of the Transantarctic
1043 Mountains deduced from sandstone detrital modes in CRP-3 drillcore, Victoria Land Basin,
1044 Antarctica. *Terra Antarctica* 8, 481-490.
- 1045 Strogen, D.P., Bland, K.J., 2011. Hydrocarbon Risk for Drilling on the Coulman High, GNS Science
1046 Consultancy Report Volume 2011/185, GNS Science, Lower Hutt, New Zealand.
- 1047 Strong, C. P., Webb, P. N., 2000. Oligocene and Miocene Foraminifera from CRP-2/2A, Victoria
1048 Land Basin, Antarctica. *Terra Antarctica* 7, 461-472.
- 1049 Sugden, D.E., Marchant, D.R., Denton, G.H., 1993. The case for a stable East Antarctic ice sheet: the
1050 background. *Geografiska Annaler. Series A. Physical Geography* 75, 151-154.
- 1051 Sugden, D., Denton, G., 2004. Cenozoic landscape evolution of the Convoy Range to Mackay Glacier
1052 area, Transantarctic Mountains: onshore to offshore synthesis. *Geological Society of America*
1053 *Bulletin* 116, 840-857.
- 1054 Talarico, F., Sandroni, S., Fielding, C. R., Atkins, C., 2000. Variability, petrography and provenance
1055 of basement clasts in core from CRP-2/2A, Victoria Land Basin, Antarctica. *Terra Antarctica* 7,
1056 529-544.
- 1057 Talbot, H. M., Farrimond, P., 2007. Bacterial populations recorded in diverse sedimentary
1058 biohopanoid distributions. *Organic Geochemistry* 38, 1212-1225.
- 1059 The Shipboard Scientific Party, 1975a. Shipboard Site Reports: Sites 270, 271, 272. *Initial Reports of*
1060 *the Deep Sea Drilling Project* 28, 211-334.
- 1061 The Shipboard Scientific Party, 1975b. Shipboard Site Reports: Site 274. *Initial Reports of the Deep*
1062 *Sea Drilling Project* 28, 369-433.
- 1063 Tissot, B.P., Welte, D.H., 1984. *Petroleum Formation and Occurrence* (2nd ed.). Springer-Verlag,
1064 Berlin Heidelberg.
- 1065 Truswell, E.M., Drewry, D.J., 1984. Distribution and provenance of recycled palynomorphs in
1066 surficial sediments of the Ross Sea, Antarctica. *Marine Geology* 59, 187-214.

- 1067 Venkatesan, M.I., 1988. Organic geochemistry of marine sediments in Antarctic region: marine lipids
1068 in McMurdo Sound. *Organic Geochemistry* 12, 13-27.
- 1069 Vogts, A., Moossen, H., Rommerskirchen, F., Rullkötter, J., 2009. Distribution patterns and stable
1070 carbon isotopic composition of alkanes and alkan-1-ols from plant waxes of African rain forest
1071 and savanna C₃ species. *Organic Geochemistry* 40, 1037-1054.
- 1072 Warny, S., Askin, R.A., Hannah, M.J., Mohr, B.A., Raine, J.I., Harwood, D.M., Florindo, F., 2009.
1073 Palynomorphs from a sediment core reveal a sudden remarkably warm Antarctica during the
1074 middle Miocene. *Geology* 37, 955-958.
- 1075 Webb, P.N., Harwood, D.M., McKelvey, B.C., Mercer, J.H., Stott, L.D., 1984. Cenozoic marine
1076 sedimentation and ice-volume variation on the East Antarctic craton. *Geology* 12, 287-291.
- 1077 Whittaker, J.M., Müller, R.D., 2006. Seismic stratigraphy of the Adare Trough area,
1078 Antarctica. *Marine geology* 230, 179-197.
- 1079 Wilson, D.S., Luyendyk, B.P., 2009. West Antarctic paleotopography estimated at the Eocene-
1080 Oligocene climate transition. *Geophysical Research Letters* 36, L16302,
1081 doi:10.1029/2009GL039297.
- 1082 Zhou, W., Xie, S., Meyers, P.A., Zheng, Y., 2005. Reconstruction of late glacial and Holocene
1083 climate evolution in southern China from geolipids and pollen in the Dingnan peat
1084 sequence. *Organic Geochemistry* 36, 1272-1284.